PREDICTIVE ON-LINE OPERATIONAL MANAGEMENT OF V2G PARTICIPATING IN THE FREQUENCY REGULATION FOR AN OFFICE GARAGE

by

YIN GUO

Submitted in partial fulfillment of the requirements for the degree of

Doctor of Philosophy

Electrical Engineering & Computer Science

CASE WESTERN RESERVE UNIVERSITY

May, 2019

CASE WESTERN RESERVE UNIVERSITY

SCHOOL OF GRADUATE STUDIES

We hereby approve the dissertation of

Yin Guo

candidate for the degree of Doctor of Philosophy[*].

Committee Chair

Dr. Marija Prica

Committee Member

Dr. Kenneth Loparo

Committee Member

Dr. Vira Chankong

Committee Member

Dr. Cenk Cavusoglu

Date of Defense

Feb 18, 2019

[*]We also certify that written approval has been obtained

for any proprietary material contained therein.

TABLE OF CONTENTS

LIST OF TABLES

LIST OF FIGURES

LIST OF ACRONYMS

AGC   Automatic generation control

EV   Electric vehicle

FT   Proposed three-stage stochastic linear programming model with fixed-length time frame for stochastic parameters

HN   Conventional multi-stage stochastic linear programming model

ISO   Independent system operator

KKT   Karush-Kuhn-Tucker conditions

MV   Simple linear programming model with the mean value of the estimated parameters

PH   Proposed three-stage stochastic linear programming model

PI   Simple linear programming model with the perfect information about parameters

PJM   Pennsylvania-New Jersey-Maryland Interconnection

SEE   Standard error of estimate

SOC   State of charge

V2G   Vehicle-to-grid

YM   Simple linear programming model with the parameters estimated by using yesterday's value

NOMENCLATURE

Symbol	Definition	Property
A^1_j, A^2_j	Constant terms in the constraints of Sub-problems 1 and 2 for j_{th} scenario	General notation
$C^R(h)$	Total frequency regulation credit of hour h	
$C^C(h)$	Frequency regulation capability credit of hour h	
$C^P(h)$	Frequency regulation performance credit of hour h	
$C^E(h)$	Energy cost of hour h	
$d_{i,act}(t)$	Final actual charge or discharge signal of time interval t for the i_{th} vehicle	
$D(h)$	Hourly average frequency regulation signal of hour h	
$f(\mathbf{x})$	Objective function of a general optimization problem	
$\mathbf{g(x)}$	Constraint functions of a general optimization problem	
$\mathbf{J}_1, \mathbf{J}_2$	Diagonal matrix that projects $\mathbf{x}$ in $\mathbf{R}^n$ into $\mathbf{R}^1$ and $\mathbf{R}^{n-1}$	
K	Number of decision variables in a general optimization problem	
$m(h)$	Hourly integrated frequency regulation mileage of hour h	
M	Mean value of the hourly integrated frequency regulation mileage	
$P(h)$	Frequency regulation power of hour h	
$r_{t,\delta}$	Correlation between frequency regulation signals at time point t and response at time point $t+\delta$	
$R^C(h)$	Frequency regulation capability credit rate of hour h	
$R^E(h)$	Energy cost rate of hour h	

Symbol	Definition	Property
$R^P(h)$	Frequency regulation performance credit rate of hour h	General notation
$R^S(h)$	Aggregated cost rate of hour h, where $R^S(h)=R^E(h)+R^C(h)+R^P(h)M$	
W	Number of all possible π	
$\mathbf{x}$	Array of decision variables in a general optimization problem	
$x_1, x_2, ..., x_K$	Elements of $\mathbf{x}$	
$x(h)$	The portion of maximum power used to charge the i_{th} EV for driving during hour h; unitless	
λ	Fritz-John multiplier	
$\boldsymbol{\lambda}$	Vector of Fritz-John multiplier	
η	Actual performance score	
$\eta_c(t)$	Correlation score at time point t	
$\eta_d(t)$	Delay score at time point t	
$\eta_p(t)$	Precision score at time point t	
ε	Error between frequency regulation signal and response	
δ	Time lag	
$Profit_{EV}(h)$	Total profit earned by an EV of hour h	
$Profit_{AG}(h)$	Total profit earned by the aggregator of hour h	
h	Hour of the day	Index
i	Vehicle number	
j	Scenario number	
t	Time interval when a frequency regulation signal is broadcasted	

Symbol	Definition	Property
$d(t)$	Original frequency regulation signal broadcasted by the grid operator at time t	
$d_{adj}{}^*(t)$	Optimal adjustment to the original frequency regulation signal for all vehicles in $\mathbf{S}(t)$	
$d^-_{adj}{}^*(t)$	Optimal adjustment to the original frequency regulation signal for all vehicles in $\mathbf{S}^-(t)$	
$d^+_{adj}{}^*(t)$	Optimal adjustment to the original frequency regulation signal for all vehicles in $\mathbf{S}^+(t)$	
$D_{PI}(h)$	Actual hourly average frequency regulation signal of hour h	
E_{max}	Maximum energy that can be stored in a single EV	
H	Hour of the day, target hour	
$H_{i,pi}$	The first whole hour after the i_{th} EV's arrival, e.g. if a vehicle joins the aggregator any time between 10:00:01 and 11:00:00, $H_{i,pi}$=11	Deterministic parameter
$H_{i,po}$	The last whole hour before the i_{th} EV's departure, e.g. if a vehicle leaves the aggregator any time between 16:00:00 and 16:59:59, $H_{i,po}$=15	
$n(h)$	Total number of available EVs under the aggregator for hour h	
N	Total number of EVs enrolled in the service of the aggregator	
N_p	Number of EVs in $\mathbf{S}^+$	
$p^*(h)$	Optimal bidding frequency regulation power capacity of the aggregator for hour h	
P_{max}	Maximum power of a single EV	
$R^S_{PI}(h)$	Actual aggregated cost rate of hour h	
$R^S_{MV}(h)$	The mean value of predicted aggregated cost rate of hour h	

Symbol	Definition	Property
$\mathbf{S}(t)$	Set of EVs, which have SOCs between $SOC_{min}+SOC_{rsv}$ and $SOC_{max}-SOC_{rsv}$ at the start of the time interval t	
$\mathbf{S}^{-}(t)$	Set of EVs, which have SOCs less than $SOC_{min}+SOC_{rsv}$ at the start of the time interval t	
$\mathbf{S}^{+}(t)$	Set of EVs, which have SOCs greater than $SOC_{max}-SOC_{rsv}$ at the start of the time interval t	
$SOC_{i,pi}$	SOC of the i_{th} EV when the vehicle joins the aggregator	
$SOC_{i,drv}$	SOC needed for one-way travel	
$SOC_{i,tgt}$	Desired SOC when the i_{th} EV leaves the aggregator	
$SOC_i(h)$	SOC of the i_{th} EV at the start of hour h	
SOC_{min}	Minimum allowable SOC	
SOC_{max}	Maximum allowable SOC	Deterministic parameter
SOC_{rsv}	Pre-defined SOC which is reserved to buffer the forced-charged energy	
T	Total number of time intervals when a regulation signal is broadcasted in an hour	
$X_i(h)$	The portion of maximum power used to charge the i_{th} EV for driving during hour h which already realizes; unitless	
ω	Random vector of the uncertainty for the information of hour H and before	
Ω	Set of all possible realization of ω	
π	Random vector of the uncertainty for the information after hour H	
Π	Set of all possible realization of π	
$D_{\omega}(h)$	Hourly average frequency regulation signal of hour h for a given ω	Stochastic parameter

Symbol	Definition	Property
$D_\pi(h)$	Hourly average frequency regulation signal of hour h for a given π	Stochastic parameter
$P^A_\omega(h)$	Actual available frequency regulation power capacity to the aggregator from all EVs for the hour h	
$R^S_\omega(h)$	Predicted aggregated cost rate of hour h for a given ω	
$R^S_\pi(h)$	Predicted aggregated cost rate of hour h for a given π	
$R^{,S}_\pi(h)$	Modified aggregated cost rate, equals to $R^S(h)/(1- D(h))$	
$R^{S+}_\omega(h)$	Aggregated punitive cost rate of hour h for the difference between the bidding and the actual available power capacity for a given ω, if the bidding power capacity is greater than the actual available power capacity	
$R^{S-}_\omega(h)$	Aggregated punitive cost rate of hour h for the difference between the bidding and the actual available power capacity for a given ω, if the bidding power capacity is less than the actual available power capacity	
$x^*_{i,\omega}(h)$	Optimal operation schedule of i_{th} EV for hour h with a given ω, obtained from the scheduling model for individual vehicle	
x_i^{PI}	The portion of maximum power used to charge the i_{th} EV for driving during hour h in PI model; unitless	Decision variable
x_i^{MV}	The portion of maximum power used to charge the i_{th} EV for driving during hour h in MV model; unitless	
$x_{i,\omega}^{HN}$	The portion of maximum power used to charge the i_{th} EV for driving during hour h with a given ω in HN model; unitless	
$x_{i,\pi}^{HN}$	The portion of maximum power used to charge the i_{th} EV for driving during hour h with a given π in HN model; unitless	
$x_{i,\omega}^{PH}$	The portion of maximum power used to charge the i_{th} EV for driving during hour h with a given ω in PH model; unitless	
$x_{i,\pi}^{PH}$	The portion of maximum power used to charge the i_{th} EV for driving during hour h with a given π in PH model; unitless	

Symbol	Definition	Property
$x_{i,\omega}^{FT}$	The portion of maximum power used to charge the i_{th} EV for driving during hour h with a given ω in FT model; unitless	Decision variable
$x_{i,\pi}^{FT}$	The portion of maximum power used to charge the i_{th} EV for driving during hour h with a given π in FT model; unitless	
$y_{i,\omega}^{HN}$	SOC of the i_{th} EV at the start of hour h with a given ω in HN model; unitless	
$y_{i,\pi}^{HN}$	SOC of the i_{th} EV at the start of hour h with a given π in HN model; unitless	
$y_{i,\omega}^{PH}$	SOC of the i_{th} EV at the start of hour h with a given ω in PH model; unitless	
$y_{i,\omega}^{FT}$	SOC of the i_{th} EV at the start of hour h with a given ω in FT model; unitless	
$Q_i^{HN}(x(h),y(h))$	Expected value function of total cost for charging the vehicle and for the failure of the i_{th} EV to provide regulation service from hour h until the EV plugs-out in HN model for given $x(h)$ and $y(h)$	Expected value function
$Q_i^{PH}(x(h),y(h))$	Expected value function of total cost for charging the vehicle and for the failure of the i_{th} EV to provide regulation service from hour h until the EV plugs-out in PH model for given $x(h)$ and $y(h)$	
$Q_i^{FT}(x(h),y(h))$	Expected value function of total cost for charging the vehicle and for the failure of the i_{th} EV to provide regulation service from hour h until the EV plugs-out in FT model for given $x(h)$ and $y(h)$	

ACKNOWLEDGEMENTS

I would like to acknowledge my family for their consistent love, encouragement and support of me during my study and research at Case Western Reserve University. Without them, I would not be able to achieve my success in study and research.

I would love to sincerely appreciate Dr. Marija Prica for her service, support and advice which have continued throughout my graduate study and research at the Case Western Reserve University. Her suggestions, assistance and all the efforts would become a great source of inspiration of my work and part of my precious experience.

I also would like thank my committee members, Dr. Kenneth Loparo, Dr. Vira Chankong and Dr. Cenk Cavusoglu, for their suggestions and contribution to my dissertation.

Predictive On-Line Operational Management of V2G

Participating in the Frequency Regulation for an Office Garage

Abstract

by

YIN GUO

The development of vehicle-to-grid (V2G) technology offers potential benefits to both electric vehicle owners and grid operators by providing frequency regulation service. Such benefits could be significant, because the vehicles are usually idle for most of the time in a day. However, it is difficult to maximize such benefits via cost-optimized on-line scheduling based on predictive real-time prices. First and foremost, this is due to the uncertainty of actual prices and the variability of prediction obtained at different time points. In addition, the energy needed for providing regulation service is unknown when making the schedule. Second, in order to participate in the frequency regulation market, an aggregator is usually needed as an interface between vehicles and grid operators. However, the optimal bidding capacity for the aggregator may conflict with the optimal schedule of individual vehicles. Last, the vehicle's ability to gain maximum profit is limited when the battery's state of charge (SOC) is close to its extreme values.

To overcome those limitations, this thesis proposes a new tool for the operational management of V2G frequency regulation. The proposed tool integrates: 1) a cost-optimized predictive on-line scheduling model for individual vehicles, 2) a cost-optimized frequency regulation capacity bidding model for an aggregator, and 3) a real-time synergetic dispatch model. The scheduling

model for individual vehicles is formulated as a three-stage stochastic linear program which considers the uncertainties in 1) energy and frequency regulation prices, and 2) hourly average frequency regulation signal.

The advantages of the proposed tool are: 1) the proposed tool properly integrates scheduling, capacity bidding and real-time dispatch; 2) the proposed scheduling models for individual EVs and the aggregator are on-line scheduling models which take the advantage of the most recent predicted electricity prices; 3) the proposed scheduling models for individual EVs and the aggregator forms a semi-centralized scheduling schema, which overcomes the disadvantages of centralized and decentralized models; 4) the consideration of the stochastic property of the parameters helps reduce the risk associate with the uncertainty, and also increase the potential profit; 5) the proposed three-stage stochastic linear programming model for the scheduling of individual vehicles greatly reduces the computational effort required by a conventional multi-stage model; 6) the proposed heuristic solution method with the utilization of GPU for parallel computation can significantly further increase the computational efficiency; 7) the proposed real-time synergetic dispatch can properly maintain the battery's SOC within a designated range, which insures that the battery energy constraint can be eliminated from the scheduling model, and helps reduce the complexity of the scheduling model.

The proposed tool is evaluated via a simulation of an arbitrary aggregator for an office garage which consists of 100 EVs. The simulation result shows that the proposed integrated tool is suitable for practical deployment.

CHAPTER 1

INTRODUCTION

1.1   Background and Motivation

With the growing concerns about global warming, sustainable energy systems—such as wind farms and solar panels—have been developing fast in the past decade. It is reported that 700 gigawatts of power will be generated by sustainable energy systems by the year 2020, which is equal to a 26% share of global power generation [1]. Due to the importance of sustainable energy systems, increasing attention has been drawn from researchers on the topics of developing new models for the control and scheduling of such energy systems for a variety of purposes.

The electric vehicle (EV) is one of those sustainable systems that could help reduce CO_2 emissions [2]. In the narrow sense, an EV refers to a type of passenger car that uses the energy from the self-contained battery and electric motors for propulsion. In the general and broad definition, EV also includes electric rail trains, surface and underwater vessels and electric aircrafts. Besides on-board battery, they may also use an on-board generator for power generation, such as solar panels or fuel cell. In this thesis, EVs are defined as a passenger car powered by an on-board battery. The definition also includes plug-in hybrid passenger cars.

EVs can achieve zero CO_2 emission via charging the battery by using the electricity generated by other renewable generation units, such as solar panels and wind turbines. However, because the EVs are charged by consuming energy from the power system and not all the energy is generated by renewable generation units, in reality the CO_2 emissions caused by the EVs are not zero and

depend on the constitution of electricity sources. Thus, the reduction in CO_2 emissions varies among locations. But despite that, the EVs have still a lower global warming emission than the conventional internal combustion motor vehicles as for nationwide [3].

In the past decade, the sales volume of EVs has been increased significantly. Figure 1 shows the EV sales volume from 2008 to 2018. It is also reported that the penetration of EVs in 13 US regions may grow to 25% by the year 2020 [4].
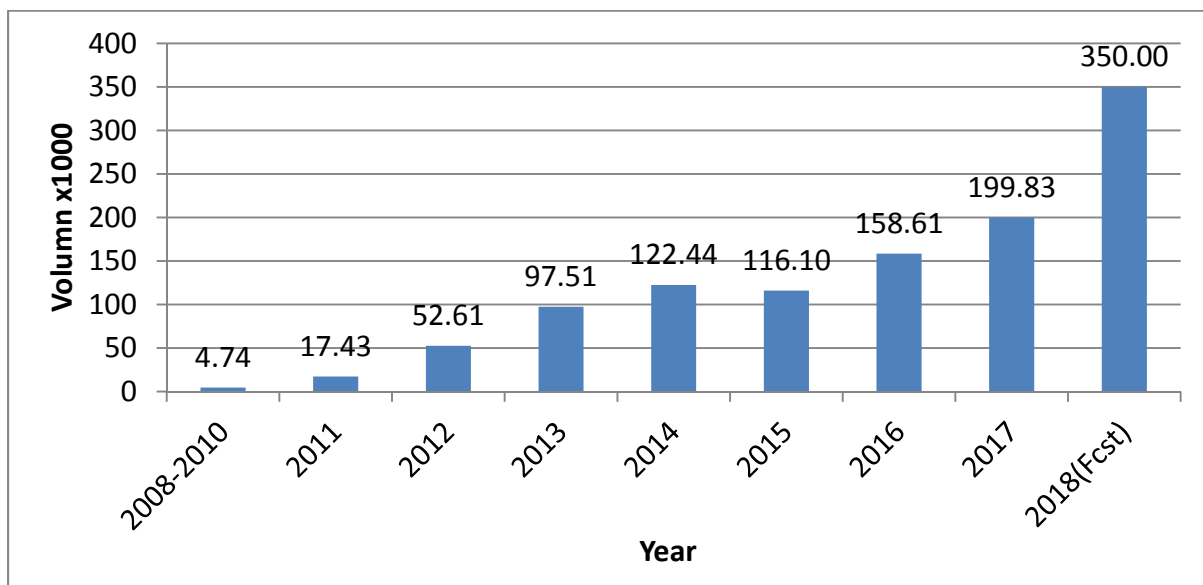
Source: insideevs.com

Figure 1 EV sales volume in the United States

As the EV market keeps expanding rapidly, technologies related to EVs are also developing at a fast pace. One of these technologies is known as vehicle-to-grid (V2G). While the traditional charging stations only allow one-directional energy flow: power grid to EVs, the current V2G charging station enables bidirectional energy exchange between EVs and the power grid. This technology allows EVs not only to consume energy from the power grid to charge the battery for driving, but also to provide energy or ancillary services back to the power grid [5]. In other

2

words, with V2G technology, EVs can function as either an ordinary load or a mobile generation unit.

The energy and ancillary services provided by EVs through V2G are beneficial to both vehicle owners and the power grid operator—they bring profit to the vehicle owners and help improve the economics, stability and reliability of the power grid. More importantly, such benefits brought by V2G could be significant, because EVs are parked in garages and plugged in for an average of 22 hours per day [6]. Therefore, taking the most advantage of those idle vehicles during such a significant period of time becomes attractive for both vehicle owners and grid operators. Thus it has drawn great attentions from researchers in the past decade.

However, traditional energy and ancillary services through V2G, such as peak load shifting, are proven to be uneconomical, when the cost of battery's degradation is taken into consideration [5, 7-9]. Take peak load shifting for example: it requires one direction energy flow constantly for a significant period of time. Such an action requires a significant amount of energy from the battery, which leads to faster battery degradation. On the contrary, primary frequency regulation services deal with the real-time deviation of power grid frequency caused by the imbalance between power generation and demand. Since the primary frequency regulation services usually deals with the high frequency part of power imbalance, it demands much less total energy delivered or absorbed by the battery. For some cases, e,g, in the Pennsylvania-New Jersey-Maryland Interconnection (PJM) system, the mean value of such an imbalance is expected to be zero for a long period of time, such a one hour. Therefore, the primary frequency regulation services are considered to be more profitable and suitable, compared to traditional energy and other ancillary services via V2G [5, 7]. Furthermore, the characteristics of V2G technology—

3

namely its ability to respond quickly to regulation signals—makes EVs an ideal primary frequency regulator [7, 10, 11].

1.2   Introduction of Aggregator

Research in the past several years has shown the promising financial potential of V2G frequency regulation [8, 12-15]. In order to participate in the primary frequency regulation market and to realize the monetary potential, an aggregator is usually needed as an interface between grid operators and individual EVs. This is because the power supply from individual EVs is too small compared to the total power available from the power grid and is therefore negligible. Several frameworks have been proposed in previous research to implement the aggregator concept [16-17].

Generally, an aggregator should be able to accomplish several important functions. First and most importantly, the aggregator should be able to charge the batteries appropriately so that the vehicle owner's travel needs in later travel can be fulfilled. Another elementary function of the aggregator is to meet the contract requirements for providing the frequency regulation service, such as the minimum power requirement. For instance, the PJM requires a minimal power of 0.1 MW to be able to participate in the frequency regulation market.

Besides the elementary functions, advanced functions are necessary for different high-level missions. One advanced function of the aggregator is to make smart decisions for the charge schedule of each individual EV to achieve certain purposes, such as maximum profit for each individual EV. Another advanced function is the appropriate dispatch of real-time control signals to each EV in a coordinated manner. Such coordinated assignments should 1) ensure that the

aggregated frequency regulation power meets the frequency regulation tasks, and 2) be capable

of maintaining a reasonable battery state of charge (SOC) so that the maximum frequency

regulation power is always accessible.

To accomplish these functions, optimal scheduling and real-time synergetic dispatch are

necessary. As EVs are idle for most of the time in a day, aside from the time used to charge the

battery for daily travel, it is very likely that there will be ample time to provide frequency

regulation services from the EVs to the power grid and make a profit. By properly scheduling the

battery charge and the use for frequency regulation, such a profit could be potentially significant

without interfering with the vehicle owners' driving needs.

1.3   Difficulties in the Scheduling

It is important to acknowledge the difficulty associated with maximizing the profit obtained

through V2G frequency regulation. First of all, several uncertainties make the decision process

of the cost-optimized scheduling an incredibly challenging task. For example, price prediction,

including the energy cost rate and frequency regulation credit rates, is essential in order to make

optimal decisions for frequency regulation schedules. However, the uncertainty of actual prices

and the variability of prediction obtained at different time points are the first challenges that need

to be overcome. Such uncertainty and variability suggest that the actual rates would almost

always vary from the predicted values. To be specific, not only may the predicted cost rate

deviate from the actual value, but the predicted cost rate may also alter at different time points.

In addition, the total energy absorbed or delivered due to providing frequency regulation services

for a specific time period is also unknown when making the decision. Moreover, an EV's arrival

and departure times are usually random. Most importantly, making a long-term schedule (for example eight hours) under the aforementioned uncertainties is usually computationally costly and almost impossible at times.

Second, although centralized scheduling models can promise a better overall result, the fact that those models suffer from high computational cost makes them inappropriate for the scheduling problem of V2G frequency regulation, especially when the aforementioned uncertainties are considered. However, the fact that decentralized models may not be able to achieve the best overall result makes them unsuitable for deployment. This is because decentralized scheduling model aims at the maximum profit for individual vehicle, while the bidding capacity is determined for the maximum profit of all vehicles. To be specific, the optimal schedules of individual vehicles are obtained based on the information of each vehicle itself in a decentralized model. In contrast, the optimal decision of the aggregator, namely the optimal bidding capacity, is obtained based on the information of all available vehicles. Therefore, the optimal decisions of individual vehicles may disagree with that of the aggregator for all vehicles in a decentralized model. Thus, coordination is needed to resolve the conflict of different objectives between the two parties in a decentralized scheduling model.

Last, without an intelligent dispatch, a vehicle's ability to gain maximum profit could be limited. This is because the optimal scheduling of an individual vehicle usually uses the hourly average regulation signal [18-21]. However, the average regulation signal from the start point of that hour to a certain time point within that hour could be significantly different from the hourly average regulation signal. Thus, at that certain time point, the vehicle's battery could have been empty or

full and therefore the vehicle becomes unavailable for providing frequency regulation services. Such challenges have already caught researchers' attention [22-24].

Lastly, most existing research focuses on only one topic in scheduling, capacity bidding or real-time dispatch [10-26]. However, the integration between the three parts has not been well studied.

1.4   Proposed Solution

To overcome these limitations, a new tool for the operational management of V2G frequency regulation is proposed in this thesis. The proposed tool integrates three sub-models: 1) a cost-optimized predictive on-line scheduling model for individual EVs, 2) a cost-optimized stochastic model for the capacity bidding of an aggregator, and 3) a real-time synergetic dispatch model. The scheduling model for individual EVs considers the uncertainties in 1) the energy cost rate and frequency regulation credit rates, and 2) the hourly average frequency regulation signal. To reduce the high computational cost that the proposed stochastic scheduling model encountered, a solution algorithm with the utilization of GPU for parallel computation is introduced. Moreover, the proposed capacity bidding model coordinates the different interests between the aggregator and the individual vehicles. Lastly, the real-time synergetic dispatch model can appropriately dispatch control signals to each individual EV in order to prevent battery from extreme SOCs and unavailability for frequency regulation service.

The features of the proposed model are as follows.

First, the proposed tool proper integrates scheduling, capacity bidding and real-time dispatch, while such integration between the three parts has not been will studied in the existing research.

Second, the proposed scheduling models for individual EVs are on-line scheduling models which focus on the determination of the nearest future planning period. Because the models take the advantage of the most recent predicted electricity prices, they can guarantee that the schedule of each period is generated with the most reliable information at the time when the schedule is made.

Third, the proposed scheduling models for individual EVs and the capacity bidding model for the aggregator forms a semi-centralized scheduling schema. It overcomes the disadvantages of centralized and decentralized models: it coordinates the schedules of individual vehicles, and reduces the computational difficulty. Therefore, it can improve the reliability of the scheduling decision when comparing with a decentralized model.

Fourth, the consideration of the stochastic property of the parameters helps reduce the risk associate with the uncertainty. Thus, such consideration can not only further improve the reliability of the scheduling decision, but also increase the potential profit.

Fifth, the proposed three-stage stochastic linear programming models for the scheduling of individual vehicles requires less computational effort compared with a conventional multi-stage model. In addition, such a modeling form better fit with the characteristic of on-line scheduling schema: it focus on the most nearest future period's schedule. Moreover, by applying a fixed-length time frame for the consideration of stochastic parameters, the computational complexity of the scheduling problem is reduced again, while it would not result in a significant worse solution.

Sixth, the proposed heuristic solution method with the utilization of GPU for parallel computation can significantly further improve the computational efficiency.

Last, the proposed real-time synergetic dispatch model can properly maintain the battery's SOC within a designated range, which insures that the battery energy constraint can be eliminated from the scheduling model. It can help reduce the complexity of the scheduling model, without requiring a significant extra burden. In addition, such a smart dispatch of control signals to each individual EV can help improve the EVs' reliability to provide frequency regulation services.

This thesis is structured as follows. A survey of existing research is reviewed in Chapter 2. System models are presented in Chapter 3. The proposed problem formulation is then developed in Chapter 4. The simulation results are presented and discussed in Chapter 5, while the conclusions are drawn in Chapter 6.

CHAPTER 2

LITERATURE REVIEW

With the rapid development of the EV market, more and more researchers focus on the optimization problems of EVs' operation. Those problems usually can be classified into four major categories: optimal vehicle charging, integration with other renewable generation resources, integration with micro-grid or smart grid, and last ancillary services via V2G.

Optimal vehicle charging problems was the first research area that caught the researcher's attention, because this problem usually does not require that the charging station has to be a V2G charging station. Numerous researches about the optimal charging problems of EVs have been reported in the past decade [25-35]. These researches aimed at the minimal charging cost for EVs through the determination of optimal charging schedule.

Along with the fast development of other renewable energy generation systems, such as wind farm or solar panel, some research focused on the integration of those systems and EVs to improve the energy outflow from the integrated system [26-27, 36-50]. Since the amount of energy generated from those systems are not stable and usually depends on many factors, EVs are used as buffer to stabilize the energy outflow from the integrated system.

In the mean time, some researchers studied the impact of EVs in a micro-grid or smart grid system. Various models have been proposed to improve the economics, reliability and stability of the micro-grid or smart grid system [27-32, 47-54].

The last group the researchers took the advantage of V2G technique, and utilized the EVs to participate in different ancillary services [54-73]. Primary frequency regulation has been the main focus of those researchers, because it has the most promising financial benefits. Usually, the proposed models can be classified into two categories depending on the solution scheme – decentralized and centralized methods.

2.1   Decentralized Scheduling Models

The decentralized scheduling models focus on the determination of the optimal schedule for one individual vehicle based on the information of the vehicle itself. They do not have or consider the information from other vehicles. However, the computation does not necessary have to be performed in a distributed manner – at the charging stations for each vehicle. As a matter of fact, the schedule can be computed by the server at the aggregator either one vehicle by one vehicle or in parallel.

S. Han et al. first developed a discrete dynamic programming model for the decentralized scheduling of V2G frequency regulation [74]. Optimal charge and frequency regulation sequence charts were generated for practical operations based on profiles of historical energy and frequency regulation prices. Later on, the energy constraint for V2G frequency regulation was further discussed when the stochastic characteristic of regulation signals was considered [18]. The stochastic characteristic was described as a random walk process with an approximated Bernoulli distribution. A quadratic programming model was then directly developed from their previous work to produce a better result [19]. It was assumed that the power capacities for regulation down and up could be different in their new model, while those two power capacities

had been assumed to be identical in their previous model. In addition, the SOC deviation caused by frequency regulation, which they had not considered in their previous work, was also taken into account in their new model. A linearly degrading weight function was used in their models to prevent battery over-charge. However, such a function restricted the EV's regulation power capacity when the battery SOC was not far from its extreme values. Thus, the EVs' ability to achieve a higher profit was still limited in their models.

Although Han's work provided a solution for the scheduling problem of V2G frequency regulation, their models did not consider several uncertainties related to the scheduling problem in real-world situations. First, the rates were from the day-ahead market and therefore assumed to be known in their model. In addition, EVs can start to provide regulation services immediately when they are plugged in. However, such assumptions are not reliable in real-world practice. This is because not all prices are available in the day-ahead market. For example, PJM has a day-ahead market for energy, but the frequency regulation service market at PJM is a real-time market. In addition, ISOs usually require the regulator to submit the frequency regulation service bid in advance, including the price and capacity. For example, PJM requires the market participator to submit the bid to PJM an hour ahead of when the target service hour begins. After that time point, the frequency regulation service market prices are settled based on the bids from all suppliers and the total power capacity needed. In other words, the V2G frequency regulation operation scheduling of individual vehicles as well as the capacity bid of the aggregator need to be made without the knowledge of the actual market prices. Moreover, this schedule should be generated even before the vehicle is plugged in, so that the frequency regulation or battery charge can be performed in a timely manner. Lastly, the uncertainty in the hourly average

regulation signal, which caused SOC deviation when providing frequency regulation, was also not well considered in their model.

To overcome some of those drawbacks, J. Donadee and M. Ilic first proposed a stochastic dynamic programming algorithm for the scheduling problem with a one-hour planning horizon [20]. The stochastic characteristic of the SOC deviation caused by frequency regulation was examined at five-minute intervals. The main drawback of this model is that the planning horizon is too short. It may lose the broad view and cannot guarantee maximum profit for the entire plugged-in period. Later on, they expanded the planning horizon, and thus the scheduling problem became a Markov decision problem [21]. A new stochastic dynamic programming algorithm was developed to heuristically solve the Markov decision problem where the cost of the subsequent time period was estimated by a piecewise linear convex function. However, the battery discharge was not allowed in their model. This constraint prevented vehicles from achieving a higher profit.

In addition, their model considered the hourly average regulation signal for a certain hour and the energy and regulation prices for the same hour in the same stage. This is inappropriate in real-world practice, and those stochastic parameters should be considered at different stages. This is because the energy and frequency regulation prices become certain at the start of that hour, while the hourly average regulation signal is realized at the end of that hour, or namely the start of the next hour. Therefore, if they are considered within the same stage, the execution of operation will be unknown at the start of that hour. This is because the information of the hourly average regulation signal for that hour is not accessible at that time. Thus, the hourly average regulation signal should be considered in a later stage.

13

E. Yao et al. first proposed a V2G frequency regulation algorithm based on robust optimization. Their model examined the influence on revenue for following regulation signals under the performance-based compensation paradigm [22]. Later, a risk-averse model was developed for the optimal day-ahead contract of V2G frequency regulation for an aggregator with the consideration of uncertain capacity due to unknown arrival and departure times of a particular EV [23]. After that, a new V2G frequency regulation algorithm based on chance-constrained robust optimization was developed directly from their previous work to produce an optimal bid [24]. By combining their previous work, a two-step algorithm was developed for EV scheduling and capacity bidding in a day-ahead market with consideration of uncertainties in vehicle's availability, market price, regulation signal. The first step used a decentralized stochastic program for EV scheduling. Given the result from the first step, the second step used another stochastic program to determine the bidding capacity. However, the proposed algorithm suffers from high computational burden, which requires powerful cloud computing.

Although extensive research has been reported on the decentralized scheduling method for the V2G frequency regulation for individual EVs, one common issue of decentralized scheduling models is that they did not consider the aggregator's obligation of proposing regulation bidding capacity. In addition, little has been discussed about the relation and coordination between the optimal bidding capacity of an aggregator and the optimal schedule of individual EVs in a decentralized model.

To achieve the maximum profit, the aggregator needs to decide the optimal bidding capacity which is going to be submitted to the ISO. For those models using day-ahead market prices or the mean values of the predicted real-time market prices, the optimal bidding capacity is the sum

of available capacity from all vehicles, because for each hour there is only one operation decision for each vehicle. However, for those models which considered the uncertainties involving the operation, such a decision is made on the premise of uncertain prices, and there is a risk that it may conflict with the operation schedule of individual EVs. Because for each hour there will be several operations decision for each possible realization of uncertain parameters for each vehicle, it is necessary in this case for the aggregator to propose a proper bidding capacity considering the available capacity from all vehicles for all possible realizations.

If the aggregator's bidding capacity is less than the total capacity available from all EVs for a certain hour, the aggregator and all EVs are losing profit, because they lose the opportunity of making higher profit in that hour. If the aggregator's bidding capacity is more than the total capacity available, then the aggregator needs to buy capacity usually at a higher rate from other regulators to fulfill the contract with the ISO or pay a penalty to the ISO for the failure of fulfilling the contract. Either way, both the aggregator and EVs are losing profit. Therefore, the coordination between the bid of an aggregator and the operation schedule of individual EVs is important.

2.2 Centralized Scheduling Models

Aside from the decentralized scheduling approach mentioned above, several models were proposed through a centralized scheduling approach. A centralized scheduling model focuses on the determination of the optimal schedules for all participating vehicles as well as the optimal bidding capacity for the aggregator based on the information from all vehicles. Different from a

decentralized scheduling model, a centralized scheduling model usually cannot be computed in a distributed manner.

E. Sortomme and M.A. El-Sharkawi proposed a linear programming model to generate the optimal schedule of individual EVs and optimal bid of the aggregator at the same time [75]. The costs of energy and battery degradation were considered in this model along with the revenue for frequency regulation and spinning reserve. M. G. Vaya and G. Andersson proposed a day-ahead scheduling model for a micro-grid to minimize the total cost of electricity generation from all generation units [76]. R. Wang et al. proposed a centralized on-line scheduling model based on the mean value of predicted prices with a moving window of a fixed length of time [77]. J. J. Escudero-Garzas et al. proposed and discussed several schemes for the aggregator to achieve maximum profit via V2G frequency regulation [78]. In their model, different criteria were implemented to achieve different degrees of fairness among EVs when allocating power to each EV. However, because centralized scheduling approaches usually require higher computational power and memory, all existing centralized scheduling models are based on the mean value of predicted prices. Therefore, these models do not account for the stochastic characteristic of prices or the hourly average regulation signal.

Although centralized scheduling models can promise a better overall profit than decentralized models by generating the schedules for individual vehicles and the bidding capacity for the aggregator simultaneously, the fact that they suffer from higher computational cost makes them unsuitable to handle the uncertainties mentioned in the previous section.

2.3   Integration of Scheduling, Capacity Bidding and Real-time Synergetic Dispatch

Most existing research focuses on only one topic in scheduling, capacity bidding or real-time dispatch, while the existing research on operation scheduling of V2G frequency regulation hardly considers the importance of the integration with capacity bidding and real-time dispatch.

As mentioned above, without a proper integration with capacity bidding, a decentralized scheduling model is not appropriate for deployment, because of the conflict of different objectives between individual EVs and the aggregator. Although a centralized scheduling model can properly resolve the conflict, the fact that it suffer from high computational cost makes it unsuitable for deployment when uncertainties are considered. Therefore, proper integration of scheduling and capacity bidding is necessary.

On the other hand, without a proper integration with real-time synergetic dispatch, not only the ability of EVs to achieve the best profit could be limited, but also the battery could be over-discharged and over-charged. However, if there are other EVs providing frequency regulation that have a much lower battery energy level, the regulation tasks that cannot be accomplished by the EVs with full batteries can be shifted to those EVs with lower battery energy levels. Furthermore, the full batteries can be actively discharged by proper signal assignments in certain situations. Thus, the battery over-discharge and over-charge of that particular EV could be avoided without reducing the frequency regulation power capacity. The synergy of an aggregator's ability to dispatch control signals to EVs in a coordinated manner makes this operation possible. Therefore, appropriate integration of scheduling and real-time synergetic dispatch is also necessary.

CHAPTER 3

SYSTEM MODELS

This chapter presents the structure of the V2G frequency regulation system, the frequency regulation compensation model, and the randomness of frequency regulation signals.

3.1   V2G Frequency Regulation System

The general architecture and information flow of a V2G frequency regulation system is shown in Figure 1. The main components of such a system are EVs, an aggregator, and an ISO. Although an aggregator can be connected to another aggregator in practice, such cases are not discussed in this thesis. This is because a child aggregator in such a scheme is mostly used in the exchange of information. Therefore, the EVs which are connected to such a child aggregator are equivalent to being connected directly to the root aggregator.

As a participant in the frequency regulation market, also known as a regulator, the aggregator needs to submit the bid to the ISO at some time point. Such a bid, including prices and capacity, is usually submitted prior to when the target service hour begins. For example, as mentioned above, PJM requires all regulators to submit their bid at least an hour before the target service hour starts. After receiving the bids from all available regulators, the ISO will select a certain number of regulators with the lowest bidding prices until the sum of their bidding capacities meets the total frequency regulation capacity needed by the grid. Thus, the frequency regulation market is settled and all selected regulators will be paid by the highest bidding prices from those selected regulators. Then, the ISO will inform the aggregator of the contract prices and capacity.

During the target service hour, the ISO will also send real-time regulation signals to the aggregator. In addition, as an energy consumer, the aggregator will also be informed of the energy price for charging EVs.
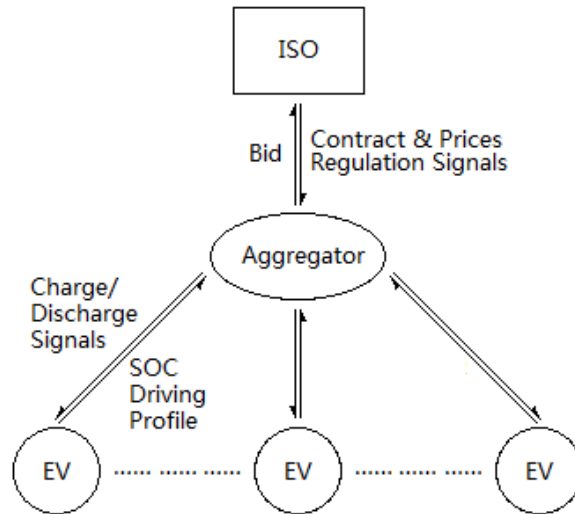
Figure 1 General framework of the V2G frequency regulation system

On the other hand, the aggregator also needs to communicate with each individual EV. Such communication includes constant queries of an EV's SOC and a one-time query of an EV's driving profile when the EV joins the aggregator. The driving profile of an EV consists of arrival and departure times, SOC at arrival, and desired SOC at departure. After collecting information from the EVs, the cost-optimized charge schedule for each EV is generated based on the predicted real-time frequency regulation credit rates and the energy cost rate. With other charge schedules, the aggregator determines the optimal bid to the ISO for the maximum profit. During the service hour, the aggregator will distribute real-time charge or discharge signals to each individual EV according to the charge schedule, battery status, frequency regulation contract,

and regulation signal from the ISO. The charge and discharge signals combine two parts: one is for the battery charge and the other is for the frequency regulation. However, the portion of the signal for frequency regulation may not directly follow the regulation signal broadcasted by the ISO. In other words, the real-time frequency regulation task may not evenly distribute to each EV according to its scheduled capacity for frequency regulation. Adjustments can be made based on the battery's status, priority and so on. However, the aggregated signal of all EVs should be able to fulfill the frequency regulation service contract with the ISO.

3.2   Frequency Regulation Compensation Model

Current frequency regulation compensation schemes in the industry are developed from the performance-based compensation paradigm, which was required by the Federal Energy Commission in Order 755. The performance-based compensation paradigm was introduced mainly to promote faster-ramping resources that provide frequency regulation, because the traditional capacity-based compensation methods failed to provide proper incentives to faster ramping regulators. In addition, these regulators usually have higher operation cost than other traditional regulators.

Take the frequency regulation compensation scheme of PJM, for example [79, 80]. The total frequency regulation credit consists of two parts: capability credit and performance credit. The capability credit is the product of the hourly-integrated frequency regulation power, actual performance score and frequency regulation market capability clearing price. The performance credit is the product of the hourly-integrated frequency regulation power, actual performance

score, mileage, and frequency regulation market performance clearing price. Such credits can be calculated by using the following equation:

$$C^R(h) = C^C(h) + C^P(h) = P(h)\eta R^C(h) + P(h)\eta m(h)R^P(h) \tag{1}$$

It is necessary to note that some ISOs, e.g. PJM, require symmetric frequency regulation capacity. In this situation, both regulation up and regulation down capacities are identical and participating regulators are paid based on one side capacity. On the contrary, other ISOs allow asymmetric frequency regulation capacity. In other words, regulation up and regulation down capacities can differ and participating regulators can be paid based on both sides of capacity.

The performance score, which is a scalar ranging from 0 to 1, describes how quickly and accurately the response from a regulator follows the regulation signals from ISO. It was evaluated in three aspects: correlation, delay and precision. The correlation score measures the degree of the relationship between the response and the regulation signal, while the delay score measures the point in time at which maximum correlation between the two signals is achieved. The precision score, on the other hand, measures the difference in the energy provided versus the energy requested by the regulation signal. One advantage of V2G frequency regulation, as mentioned in the previous discussion, is its ability to quickly respond to regulation signals. Therefore, both the correlation and delay scores can be considered as 1 for V2G frequency regulation. In addition, as long as there is sufficient capacity, the precision score can also be considered as 1 for V2G frequency regulation. Therefore, without losing generality, the performance score of V2G frequency regulation can be assumed to be 1. The calculation of those scores is illustrated by Eq. (2)-(5) [80].

21

$$\eta_C(t) = r_{t,t+\delta} \qquad 0 \le \delta \le 5 \min \tag{2}$$

$$\eta_d(t) = \left| \frac{\delta - 5}{5} \right| \qquad 0 \le \delta \le 5 \min \tag{3}$$

$$\eta_p(t) = 1 - \frac{1}{K} \sum_{k=1}^{K} |\varepsilon_k| \tag{4}$$

$$\eta = \frac{1}{3} \left(\max_{0 \le \tau \le 5} (\eta_c(t + \tau) + \eta_d(t + \tau)) + \eta_p(t) \right) \tag{5}$$

As shown in Eq. (6), the mileage is defined as the summation of movement requested by the regulation control signal that a resource is following [80]. In other words, it is the summation of the absolute difference between two consecutive regulation signals.

$$m(h) = \sum_{t=1}^{T} |d(t) - d(t-1)| \tag{6}$$

3.3 Randomness of Frequency Regulation Signal

The frequency regulation signal is generated from an automatic generation control (AGC) signal, where the AGC signal is the real-time mismatch between generation and load in the power grid governed by the ISO. Usually, the frequency regulation signal is the high frequency part of the AGC signal. Therefore, the time interval between two consecutive frequency regulation signals is generally very short, especially when compared with the time interval for a frequency regulation service contract. For example, in PJM, the contract commitment is for one hour, while the frequency regulation signal is broadcasted every two seconds.

The frequency regulation signal, by definition, is the real-time power mismatch in the power grid divided by the designated frequency regulation power capacity. Therefore, the frequency regulation signal has no unit. Typically, different regulators have different committed frequency regulation capacities. During a real-time operation, instead of sending different numbers of real-time charge or discharge power to different regulators, the ISO sends only one number to all regulators. Thus, the real-time frequency regulation task for a regulator is the product of the contract capacity and the frequency regulation signal. Therefore, the communication between an ISO and a regulator is simplified, and the communication reliability is improved.
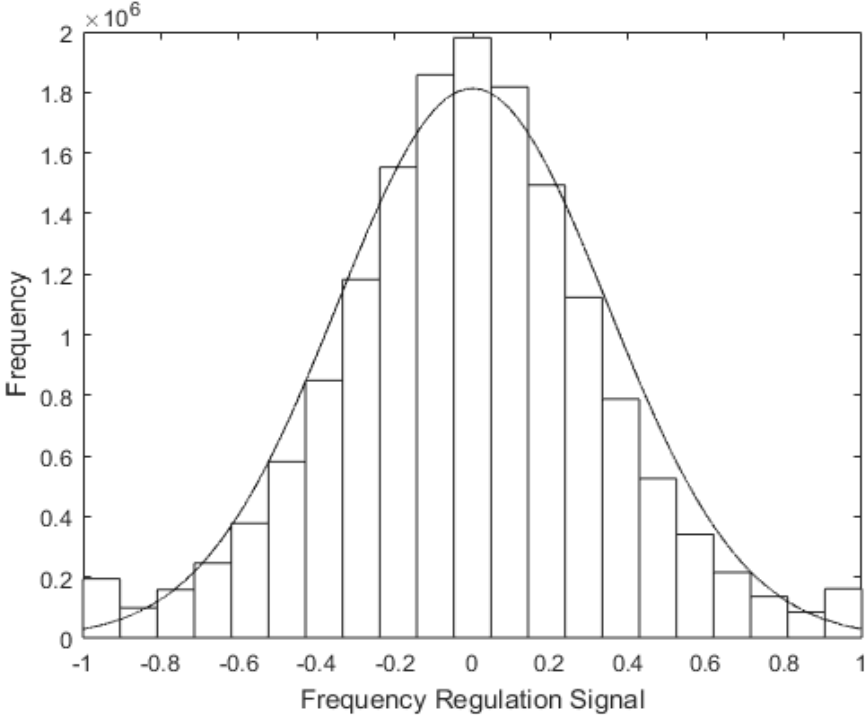
Source: pjm.com

Figure 2 Distribution of frequency regulation signals

Although the frequency regulation signal is assumed to follow normal distribution with zero mean in many models, the actual distribution of the frequency regulation signal shows otherwise.

23

Figure 2 shows the actual distribution of the frequency regulation signal broadcast by PJM from June 1 2013 to May 31 2014 [82]. Although the main part of frequency regulation signal data follows the normal distribution, the frequencies at both ends are much higher than the theoretical values according to Figure 2, because the frequency regulation signal is bounded between -1 and 1.
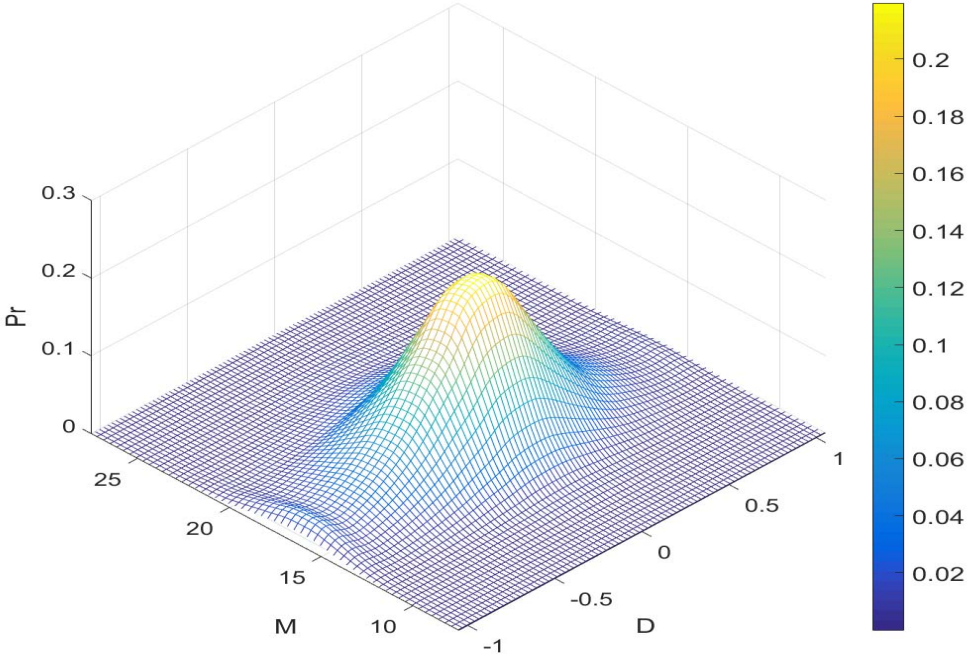
Figure 3 Histogram of frequency regulation signals

Since the frequency regulation signal is random, both the hourly average frequency regulation signal and the hourly integrated mileage are also random. Figure 3. is the 2-D histogram of the hourly average frequency regulation signal and the hourly integrated mileage generated from the same data. The distribution of the hourly average frequency regulation signal is similar to the

distribution shown in Figure 2, due to the same issue. Although the hourly average frequency

regulation signal and the hourly integrated mileage are all generated from the same data, a

correlation coefficient of 0.0010 indicates their independence.
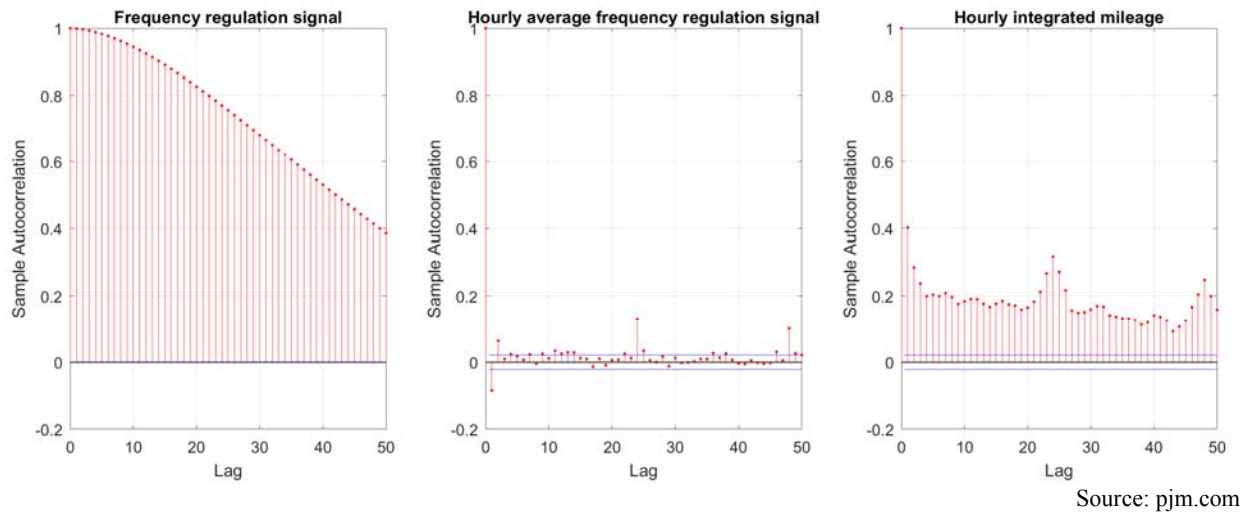
Figure 4 Histogram of frequency regulation signals

Figure 4 shows the autocorrelation of the aforementioned three signals. On one hand, the

frequency regulation signal is highly dependent on its most recent values, and such dependence

decreases gradually as time increases. On the other hand, although there is a seasonal pattern for

both the hourly average frequency regulation signal and the hourly integrated mileage, their

ability to remember their previous status differs. Specifically, the hourly average frequency

regulation signal hardly remembers its previous status, while the hourly integrated mileage has a

better memory of its past status.

CHAPTER 4

PROBLEM FORMULATION

The proposed model is developed in this Chapter.

4.1 Scheme of the Proposed Model

The proposed model contains three sub-models: 1) the on-line cost-optimized predictive V2G

frequency regulation scheduling model for individual vehicles, 2) the predictive frequency

regulation capacity bidding model for an aggregator, and 3) the real-time synergetic dispatch

model. Although the proposed models are based on the PJM market regulation and cost structure,

with small modifications, it can be implemented to other ISOs with different market regulations

and cost structures.

Figure 5 demonstrates the scheme of the proposed model.

The scheduling model for individual vehicles determine the initial operation schedules of the

individual EVs for one hour at a time based on the predicted market prices for the entire plug-in

period. The scheduling model for individual vehicles considers two aspects of stochastic

parameters: the electricity market prices and the hourly average frequency regulation signal. The

operation schedule for the hour after the current target hour will be determined at the start of the

hour following the current target time.

The initial optimal schedules of all individual EVs and the predicted electricity prices then

become the inputs for the frequency regulation capacity bidding model for an aggregator. It

determines the optimal bidding capacity of the aggregator and the intermediate operation

schedules of individual EVs. Such schedules are generated through the adjustment on the initial

operation schedule in accordance to the optimal bidding capacity of the aggregator.
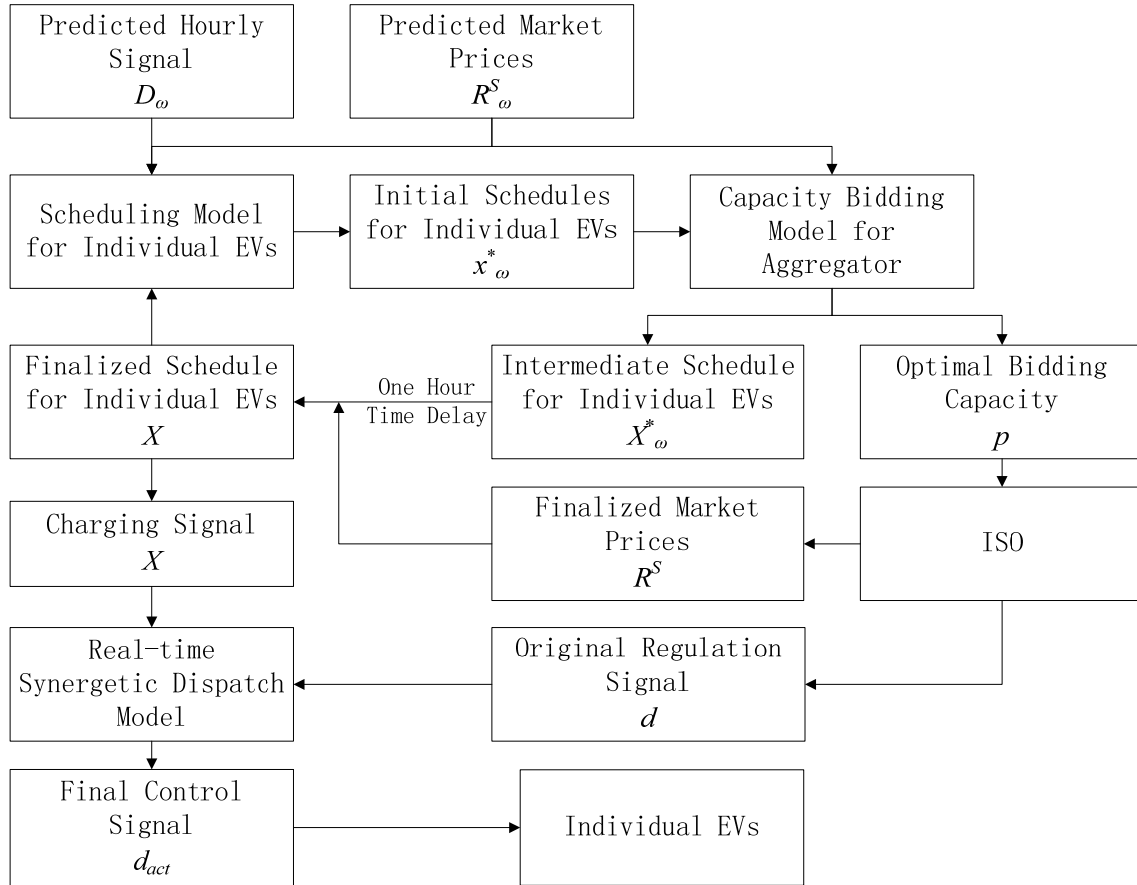
Figure 5 Scheme of the Proposed Model

After an hour's delay, as the market prices are settled, the schedule for individual EVs will be

finalized. The finalized schedules then become the input for the real-time dispatch model and

will also be used as deterministic parameter in the scheduling model for individual vehicles to

determine the operation schedule of an individual EV for the hour right after the current target

hour. The real-time synergetic dispatch model will generate the real-time control signal for each

individual vehicle based on the finalized schedule and the original regulation signal from the ISO. The dispatch model assures that the battery's SOC at any time during the plug-in period is within the designated feasible range. Therefore, it is practical to neglect the battery's energy constraints which are necessary for the optimal operation scheduling.

4.2   Assumptions

The proposed tool is designed for an aggregator of an office garage which participates in the real-time market of the PJM. As the profile of the participating EVs in an office garage environment is more stable than a residential, the EVs' arrival and departures times and the SOCs at those time points could be estimated by using historical data with a high confidence level. In addition, the arrival and departure times as well as the desired SOC at the departure could be specified in the contract agreement with the vehicle owners.

The proposed tool considers two stochastic parameters: 1) energy and frequency regulation prices, and 2) hourly average frequency regulation signal. However, since the uncertainty of vehicle's arrival and departure times have to be handled in a different way, it is beyond the scope of this paper and will be presented in our future work.

Thus, the following assumptions are made in this thesis.

- The necessary communication frame and infrastructure have been well established.
- Charge and discharge efficiency are considered to be 1.
- All vehicles have the same type of battery.
- The EVs' arrival and departures times are known.

- Maximum battery capacity and maximum battery charging and discharging rates are identical.

- The EVs' SOCs at arrival and the EVs' desired SOCs at departure are known prior to vehicles' arrival.

4.3 On-line Predictive Cost-optimized Scheduling of V2G Frequency Regulation for Individual EVs

This section develops the on-line predictive cost-optimized scheduling model of V2G frequency regulation for individual EVs. First, the simple linear programming and the corresponding multi-stage stochastic linear programming models are introduced. Then, the proposed scheduling model which is formulated as a three-stage stochastic linear program is developed. Last, a three-stage stochastic linear program with a fixed-length time window for the consideration of the stochastic parameters is elaborated for practical implementation.

The stochastic scheduling models discussed in this section consider the uncertainties in:

1) The cost rate for energy and the credit rates for frequency regulation in the real-time market

2) The total energy delivered and absorbed by the battery due to regulation service in an hour, or namely the hourly average frequency regulation signal

Basically, the profit of i_{th} EV's operation for a certain hour h can be expressed as follows.

$$Profit_{EV}(h) = C^E(h) + C^C(h) + C^P(h)$$
$$= -R^E(h)x(h) - R^E(h)(1-x(h))D(h) + R^C(h)(1-x(h)) + R^P(h)(1-x(h))m(h)$$
$$= \left(R^C(h) + R^P(h)m(h) - R^E(h)D(h)\right) - \left(R^E(h) - R^E(h)D(h) + R^C(h) + R^P(h)m(h)\right)x(h) \qquad (7)$$
$$\approx \left(R^C(h) + R^P(h)M\right) - \left(R^E(h) + R^C(h) + R^P(h)M\right)x(h)$$
$$= \left(R^C(h) + R^P(h)M\right) - R^S x(h)$$

Basically, the total profit of a vehicle's operation contains two parts. The first part, $C^E(h)$, is the cost of energy that is charged into the battery. The second part, $C^C(h)+C^P(h)$, is the credit for providing frequency regulation. The energy cost can be calculated by the first two terms in the second line of Eq. (7). The first term is for the energy needed to charge battery for driving, while the second term is for the total energy delivered and absorbed by the battery due to frequency regulation. It is necessary to note that $R^E(h)$, $R^C(h)$ and $R^P(h)$ are known at the start of hour h, while $D(h)$ and $m(h)$ are unknown until the end of hour h. Therefore, the profit of a vehicle for hour h is estimated by using the mean value of $D(h)$ and $m(h)$, which are zero and M respectively. Because the first two terms in the last line of Eq. (7) are parameters, the maximization of a vehicle's profit is equivalent to the minimization of the total cost for charging the vehicle and for the failure to provide regulation service, which is represented by the last term.

4.3.1 Deterministic Simple Linear Programming Models

According to the previous discussion, the simple linear program for the scheduling of i_{th} vehicle from H_{pi} until H_{po} based on the prefect information of the aggregated cost rate and the hourly average frequency regulation signal is formulated as follows. This model is denoted as PI model.

$$z_i = \min_{x} \sum_{h=H_{i,pi}}^{H_{i,po}} R_{PI}^{S}(h) x_i^{PI}(h) \qquad \forall i = 1, 2, ..., N \tag{8}$$

subject to:

$$SOC_{i,pi} + \frac{P_{max}}{E_{max}} \sum_{h=H_{i,pi}}^{H_{i,po}} \left[x_i^{PI}(h) + \left(1 - x_i^{PI}(h)\right) D_{PI}(h) \right] \geq SOC_{i,tgt} \tag{9}$$

$$SOC_{min} \leq SOC_{i,pi} + \frac{P_{max}}{E_{max}} \sum_{h=H_{i,pi}}^{H} \left[x_i^{PI}(h) + \left(1 - x_i^{PI}(h)\right) D_{PI}(h) \right] \leq SOC_{max}$$

$$H = H_{i,pi} + 1, H_{i,pi} + 2, ..., H_{i,po} \tag{10}$$

$$0 \leq x_i^{PI}(h) \leq 1 \tag{11}$$

The objective function, Eq. (8), calculates the total operational cost from H_{pi} until H_{po}. Eq. (9) requires that the battery's SOC when the vehicle leaves the aggregator should be greater than the desired SOC. Eq. (10) ensures that the battery's SOC at the start of each hour between H_{pi} and H_{po} should be within the feasible range. Eq. (11) defines the feasible region of the decision variable.

Because in the practical operation both the aggregated cost rate and the hourly average frequency regulation signal are unknown before they realize, PI model cannot be used for practical implementation. However, it is a suitable model for benchmarking purpose which calculates the least minimal operational cost. Any scheduling model with imperfect information cannot obtain an operational cost lower than that obtained from the PI model. The difference between the operational costs obtained from a scheduling model with imperfect information and from the PI model is defined as the cost of prefect information. The lower the cost of prefect information, the better performance the scheduling model with imperfect information has.

The simple linear program based on the mean values of the predicted aggregated cost rate and the hourly average frequency regulation signal is a practical model for the on-line scheduling of i_{th} vehicle from a certain hour H until H_{po}. This model is denoted as MV model and formulated as follows. Because the mean of the hourly average frequency regulation signal is zero, the total energy delivered and absorbed by the battery due to regulation service is zero.

$$z_i = \min_x \sum_{h=H}^{H_{i,po}} R_{MV}^S(h) x_i^{MV}(h) \qquad \forall i = 1,2,...,N \tag{12}$$

subject to:

$$SOC_i(H) + \frac{P_{max}}{E_{max}} \sum_{h=H}^{H_{i,po}} x_i^{MV}(h) \geq SOC_{i,tgt} \tag{13}$$

$$SOC_{min} \leq SOC_i(H) + \frac{P_{max}}{E_{max}} \sum_{h=H}^{H'} x_i^{MV}(h) \leq SOC_{max} \qquad H' = H+1, H+1,..., H_{i,po} \tag{14}$$

$$0 \leq x_i^{MV}(h) \leq 1 \tag{15}$$

As the objective function, Eq. (12) calculates the total operational cost from H until H_{po}. Eq. (13) ensures that the battery's SOC when the vehicle leaves the aggregator should be greater than the desired SOC. Eq. (14) ensures that the battery's SOC at the start of each hour between H and H_{po} should be within the feasible range. Eq. (15) defines the feasible region of the decision variable.

Generally, the cost of prefect information of the MV model depends on the prediction accuracy of the aggregated cost rate. The higher the prediction accuracy is, the lower the cost of prefect information is. It is also necessary to mention that because the mean value of the hourly average regulation signal is zero, participating in the frequency regulation will not affect the battery's

SOC. Therefore, only the charging process will count for the change in the battery's SOC in Eq. (13).

Specifically, a simple and straightforward estimation of future market prices is directly using the yesterday's market prices. This specific model is denoted as YM model.

4.3.2 Multi-stage Stochastic Linear Programming Model

If the uncertainties of the predicted aggregated cost rate and the hourly average frequency regulation signal are considered, a multi-stage stochastic linear program can be developed directly from the MV model. The multi-stage stochastic linear programming model is denoted as HN model and formulated as follows.

$$z_i = E_{\omega \in \Omega} \left\{ \min_{x,y} R^S_{\omega}(H) x^{HN}_{i,\omega}(H) + Q^{HN}_i \left(x^{HN}_{i,\omega}(H), y^{HN}_{i,\omega}(H) \right) \right\} \qquad \forall i = 1,2,...,N \qquad (16)$$

subject to:

$$y^{HN}_{i,\omega}(H) = \begin{cases} SOC_{i,pi} & H = H_{i,pi} \\ SOC_i(H-1) + \dfrac{P_{max}}{E_{max}} \left(X_i(H-1) + D_{\omega}(H-1)\left(1 - X_i(H-1)\right) \right) & H_{i,pi} < H \le H_{i,po} \end{cases}$$

$$(17)$$

$$0 \le x^{HN}_{i,\omega}(H) \le 1 \qquad (18)$$

where

$$Q^{HN}_i \left(x^{HN}_{i,\omega}(H), y^{HN}_{i,\omega}(H) \right) = \begin{cases} E_{\pi \in \Pi} \begin{pmatrix} \min\limits_{x,y} R^S_{\pi}(H+1) x^{HN}_{i,\pi}(H+1) \\ + Q^{HN}_i \left(x^{HN}_{i,\pi}(H+1), y^{HN}_{i,\pi}(H+1) \right) \end{pmatrix} & H < H_{i,po} \\ 0 & H = H_{i,po} \end{cases} \qquad (19)$$

and

$$Q_i^{HN}\left(x_{i,\pi}^{HN}(h), y_{i,\pi}^{HN}(h)\right) = \begin{cases} E \\ \pi \in \Pi \end{cases} \left(\begin{array}{c} \min_{x,y} R_\pi^S(h+1)x_{i,\pi}^{HN}(h+1) \\ + Q_i^{HN}\left(x_{i,\pi}^{HN}(h+1), y_{i,\pi}^{HN}(h+1)\right) \end{array} \right) \quad H < h < H_{i,po}$$
$$\qquad\qquad\qquad\qquad\qquad\qquad\qquad\qquad 0 \qquad\qquad\qquad\qquad\qquad h = H_{i,po} \tag{20}$$

subject to:

$$y_{i,\pi}^{HN}(h+1) = \begin{cases} y_{i,\omega}(h) + \dfrac{P_{max}}{E_{max}}\left(x_{i,\pi}^{HN}(h) + D_\pi(h)\left(1 - x_{i,\pi}^{HN}(h)\right)\right) & h = H \\[3mm] y_{i,\pi}(h) + \dfrac{P_{max}}{E_{max}}\left(x_{i,\pi}^{HN}(h) + D_\pi(h)\left(1 - x_{i,\pi}^{HN}(h)\right)\right) & h = H+1, H+2,..., H_{i,po} \end{cases}$$
$$\tag{21}$$

$$y_{i,\pi}^{HN}(H_{i,po}+1) \geq SOC_{i,tgt} \tag{22}$$

$$0 \leq x_{i,\pi}^{HN}(h) \leq 1 \qquad h = H+1, H+2,..., H_{i,po} \tag{23}$$

$$SOC_{min} \leq y_{i,\pi}^{HN}(h) \leq SOC_{max} \qquad h = H+1, H+2,..., H_{i,po}+1 \tag{24}$$

The objective function, Eq. (16), calculates the expected total cost for charging the vehicle and for the failure to provide regulation service from the start of hour H until the EV plugs-out. The first term in Eq. (16) represents the cost related to the operation in hour H and the second term is the expected cost due to the operation from hour $H+1$ until the EV plugs-out.

Eq. (17) calculates the SOC of i_{th} EV at the start of hour H for a possible realization of ω. Basically, $y_{i,\omega}(H)$ is equal to the sum of the SOC which is known for sure and the change of SOC caused by charging the battery and providing frequency regulation service for a possible realization of ω. For different values of H, $y_{i,\omega}(H)$ has different expressions due to the knowledge of information.

Eq. (19) and (20) calculate the expected cost due to the operation from hour $H+1$ to $H_{i,po}$. The fact that stochastic parameters realize hour by hour directly leads to the recursion of $Q(x,y)$. Thus, the HN model is multi-stage stochastic linear programming model.

The SOC at the start of every hour after H can be determined by using Eq. (21), while Eq. (22) guarantees that the SOC meets the vehicle owner's need for travel when the vehicle plugs-out.

Eq. (18), (23) and (24) define the feasible range of the decision variables.

There are several issues with the HN model. First and foremost, the model confronts extreme high computational density. It is well known that solving a multi-stage stochastic linear program is not only time costly, but also requires enormous memory to complete the calculation. This is true even if the number of possible scenarios for each stage and the number of stages are not too large. This is simply because the total number of scenarios grows exponentially as the number of stages increase. For example, if both $R^S_\omega(h)$ and $D_\omega(h)$ have five possible values for each stage, there will be a total of $25^8=5^{16}\approx1.5\times10^{11}$ possible scenarios for a vehicle whose plug-in period is eight hours. It is almost impossible to solve such a problem by using a commercial desktop. Therefore, the HN is meaningless in practice.

Second, the decision of an individual EV's schedule for hour $H+1$, $H+2$,..., $H_{i,po}$ is not so important for the on-line predictive scheduling when compared to that for hour H, but the value of $Q(x(H),y(H))$ is vital. This is because the decision for hour H is the most important for both the individual EV's operation and the aggregator's decision of capacity bidding for hour H. Once the schedule and the capacity bidding for hour H are made, they are settled, while those for hour $H+1$ and after can be revised in the future. Since the prediction of rates updates at the start of

each hour, it is more confident to decide the schedule for hour $H+1$ based on the predicted rates obtained at the next update. In addition, as mentioned in the previous discussion, both the prediction mean and distribution change between two contiguous predictions. For example, the prediction of $R(H+1)$, $R(H+2)$,…, $R(H_{i,po})$, which are generated in hour H-2, will be different from those generated in hour H-1. Therefore, the decision made at hour H-1 for the operation of hour $H+1$ is more confident than that made at hour H-2. Thus, on-line scheduling is appropriate for this problem. An on-line scheduling model focuses on making decisions for one individual time step at a time.

Third, there is no assurance that the battery's SOC is within feasible range at any time during the plug-in period. The frequency regulation signal is broadcasted at a very small time interval. For example, in PJM the signal is broadcasted every two second. Therefore, there will be thousands of battery' energy constraints for only one hour. In the meantime, the battery's SOC at a given time is determined by its previous value, schedule decision and a frequency regulation signal. The fact that the frequency regulation signal is a stochastic parameter makes the examination of battery's energy constraint at every small time interval impossible. This is why the battery's energy constraint is only examined at the start of each hour in HN model and in the literature mentioned in the previous discussion [19-21].

4.3.3   *Proposed Three-stage Stochastic Linear Programming Model*

To overcome the aforementioned drawbacks of a multi-stage stochastic linear programming model, a three-stage stochastic linear program is proposed. The proposed model is denote as PH model and formulated as follows.

36

$$z_i = \mathop{E}\limits_{\omega \in \Omega} \left\{ \min_{x,y} R_\omega^S(H) x_{i,\omega}^{PH}(H) + Q_i^{PH}\left(x_{i,\omega}^{PH}(H), y_{i,\omega}^{PH}(H)\right) \right\} \qquad \forall i = 1,2,...,N \qquad (25)$$

subject to:

$$y_{i,\omega}^{PH}(H) = \begin{cases} SOC_{i,pi} & H = H_{i,pi} \\ SOC_i(H-1) + \dfrac{P_{max}}{E_{max}}\left(X_i(H-1) + D_\omega(H-1)\left(1 - X_i(H-1)\right)\right) & H_{i,pi} < H \le H_{i,po} \end{cases}$$

$$(26)$$

$$0 \le x_{i,\omega}^{PH}(H) \le 1 \qquad (27)$$

where

$$Q_i^{PH}\left(x_{i,\omega}^{PH}(H), y_{i,\omega}^{PH}(H)\right) = \mathop{E}\limits_{\pi \in \Pi}\left(\min_{x,y} \sum_{h=H+1}^{H_{i,po}} R_\pi^S(h) x_{i,\pi}^{PH}(h) \right) \qquad (28)$$

subject to:

$$SOC_{i,tgt} \le y_{i,\omega}^{PH}(H) + \frac{P_{max}}{E_{max}}\left(x_{i,\omega}^{PH}(H) + D_\pi(H)\left(1 - x_{i,\omega}^{PH}(H)\right) + \sum_{h=H+1}^{H_{i,po}}\left(x_{i,\pi}^{PH}(h) + D_\pi(h)\left(1 - x_{i,\pi}^{PH}(h)\right)\right) \right)$$

$$(29)$$

$$0 \le x_{i,\pi}^{PH}(h) \le 1 \qquad h = H_{i,pi} + 1, H_{i,pi} + 2,..., H_{i,po} \qquad (30)$$

The objective function, which is Eq. (25), calculates the expected total cost for charging the vehicle and for the failure to provide regulation service from the start of hour H until the EV plugs-out. Eq. (26) determines the SOC of i_{th} EV at the start of hour H under the condition of a possible realization of ω. Eq. (28) calculates the expected cost due to the operation from hour $H+1$ to $H_{i,po}$. Eq. (29) requires that the SOC meets the vehicle owner's need for travel when the vehicle plugs-out. Eq. (27) and (30) define the feasible range of the decision variables.

In the proposed PH model, $Q(x(H),y(H))$ is calculated by using the wait-and-see method, while the calculation of $Q(x(H),y(H))$ in the HN model uses the here-and-now method. Those two methods are introduced, compared and discussed in [83]. The difference of the two methods is the realization time of the stochastic parameters. In the here-and-now method, the stochastic parameters realize gradually in each time period, while the stochastic parameters in the wait-and-see method realize all at once in one stage.

In the on-line scheduling situation, the proposed PH model is more appropriate. Indeed, no matter what model is used, the stochastic parameters realize gradually in each time period. However, the on-line scheduling scheme gives the decision maker the flexibility to make decisions for hours after the target hour H in a later time. On the contrary, the advantage of the HN model is that it minimizes the risk of high cost when the decision maker has to make the decision for both target hour H and hours after that all at once right before the target hour H. But those decisions will not be revised in a later time. However, the on-line scheduling scheme does not require such strict restriction, which means over-conservative. Therefore, the proposed PH model is more appropriate in the on-line scheduling situation.

Due to the proposed real-time synergetic dispatch model, the battery's energy constraint is neglected. Such neglect is feasible because: 1) based on the statistical result [84], only a small portion of EVs need to be fully charged for normal daily travel. In other words, only a small portion of EVs have SOCs close to 0 when they join the aggregator and have SOCs close to 1 when they leave the aggregator. Only those vehicles may have the chance to reach the minimum or maximum allowable energy. And only those vehicles may have limited retrievable regulation power. 2) According to Figure 2, the regulation signal rarely deviates from zero significantly:

for example below -0.6 or above 0.6. Hence, by sending charge or discharge signals to each EV

under the aggregator in a coordinated manner, vehicles that have low SOC could be actively

charged and those that have high SOC could be actively discharged, without violating the

frequency regulation service contract. 3) Because the maximum value of hourly average

frequency regulation signal is 1, the maximum change to SOC due to frequency regulation in a

single hour is $P_{\max}/E_{\max}$. Therefore, despite the possible inconvenience and loss of profit, the

battery will never get over-charged or over-discharged when $SOC_{rsv}=P_{\max}/E_{\max}$. Thus the SOC of

a battery could be maintained within a feasible range and not reach its extreme values when

providing regulation services. Therefore, the battery's energy constraint can be fulfilled and

ignored.

In addition, due to the proposed real-time synergetic dispatch model, the minimum SOC when an

EV leaves the aggregator is calculated by using the following equation.

$$SOC_{i,tgt} = \begin{cases} SOC_{\min} + SOC_{i,drv} & SOC_{i,drv} < SOC_{\max} - SOC_{\min} - SOC_{rsv} \\ SOC_{\max} - SOC_{rsv} & \text{otherwise} \end{cases} \tag{31}$$

Generally, $SOC_{i,tgt}$ is the sum of $SOC_{\min}$ and $SOC_{i,drv}$, where $SOC_{\min}$ is the minimum allowable

value below which may result in a significant reduction in battery life. Also, due to the proposed

real-time synergetic dispatch model, $SOC_{i,tgt}$ should not exceed $SOC_{\max}$-SOC_{rsv}, so that there is

still room for the forced charge energy to be stored in the battery to provide regulation services

after the charging process.

This definition of $SOC_{i,tgt}$ may cause inconvenience to vehicle owner when $SOC_{i,drv}$ is very close

to $SOC_{\max}$. At the end of $H_{i,po}$, the SOC of the battery could be slightly lower than the actual

desired SOC in this case. However, this situation is rare and can be neglected. This is because 1) the portion of the vehicle whose $SOC_{i,\text{drv}}$ is greater than SOC_{max}-SOC_{min}-SOC_{rsv} is small according to [84]; 2) since $H_{i,po}$ is the last whole hour before an EV leaves the aggregator, there will be some time to charge the battery which is less than an hour from the end of $H_{i,po}$ to the time at which an EV actually leaves the aggregator; 3) the difference between the actual desired SOC and SOC_{max}-SOC_{rsv} is small, and therefore can be charged in a short period of time.

4.3.4   *Proposed Heuristic Solution Algorithm*

Since one possible realization of ω is independent from all other possible realizations, the PH model can be first decomposed into several two-stage stochastic linear programs. In addition, the introduction of the real-time dispatch model removes the constraint that the SOC should be within the feasible range at any time point between the plug-in and plug-out times from the PH model. Such removal leaves only one constraint when calculating $Q_i(x_{i,\omega}(H),y_{i,\omega}(H))$. In addition, because the wait-and-see method calculates the expected value of a set of simple linear programs for each possible scenario, by using the wait-and-see method, the calculation of $Q_i(x_{i,\omega}(H),y_{i,\omega}(H))$ can be broken down from a huge linear programming problem to a large number of small linear programming problems, which are independent from each other. Thus, the calculation of $Q_i(x_{i,\omega}(H),y_{i,\omega}(H))$ can be then decomposed into thousands of simple linear programs, given $x(H)$ and $y(H)$ as parameters. Hence, the two-stage stochastic linear programs can be solved using decomposition method.

Therefore, the original PH model can be rewritten as follows, and it can be solved through the procedure illustrated in Figure 6.

$$z_{i,\omega} = \min_{x,y} R_\omega^S(H)x_{i,\omega}^{PH}(H) + Q_i^{PH}\left(x_{i,\omega}^{PH}(H), y_{i,\omega}^{PH}(H)\right) \qquad \forall i = 1,2,...,N \quad \forall \omega \in \Omega \tag{32}$$

subject to:

$$y_{i,\omega}^{PH}(H) = \begin{cases} SOC_{i,pi} & H = H_{i,pi} \\ SOC_i(H-1) + \dfrac{P_{max}}{E_{max}}\left(X_i(H-1) + D_\omega(H-1)(1-X_i(H-1))\right) & H_{i,pi} < H \le H_{i,po} \end{cases} \tag{33}$$

$$0 \le x_{i,\omega}^{PH}(H) \le 1 \tag{34}$$

where

$$Q_i^{PH}\left(x_{i,\omega}^{PH}(H), y_{i,\omega}^{PH}(H)\right) = E\left(\min_{x,y} \sum_{h=H+1}^{H_{i,po}} \frac{R_\pi^S(h)}{1-D_\pi(h)} x_{i,\pi}^{\prime PH}(h)\right) = E\left(\min_{x,y} \sum_{h=H+1}^{H_{i,po}} R_\pi^{\prime S}(h) x_{i,\pi}^{\prime PH} h\right) \tag{35}$$

subject to:

$$SOC_{i,tgt} \le y_{i,\omega}^{PH}(H) + \frac{P_{max}}{E_{max}}\left(x_{i,\omega}^{PH}(H) + D_\pi(H)(1-x_{i,\omega}^{PH}(H)) + \sum_{h=H+1}^{H_{i,po}} D_\pi(h) + \sum_{h=H+1}^{H_{i,po}} x_{i,\pi}^{\prime PH}(h)\right) \tag{36}$$

$$0 \le x_{i,\pi}^{\prime PH}(h) \le 1 - D_\pi(h) \qquad h = H_{i,pi}+1, H_{i,pi}+2,..., H_{i,po} \tag{37}$$

Based on Eq. (36)-(37), since the contribution of each $x'_{i,\pi}(h)$ to the battery's final SOC is equivalent, the greedy algorithm can be implemented to solve the small simple linear programs after the decomposition by selecting the $x'_{i,\pi}(h)$ with lowest $R^S_\pi(h)$ to fulfill the charge demand. Because current GPU contains thousands of cores, compared with 2-16 cores in CPU, the parallel computation of $Q_i(x_{i,\omega}(H), y_{i,\omega}(H))$ becomes very efficient when performed on GPU. Thus, the utilization of GPU for parallel computation is very suitable and efficient in solving such simple linear programming problems by using the greedy algorithm.
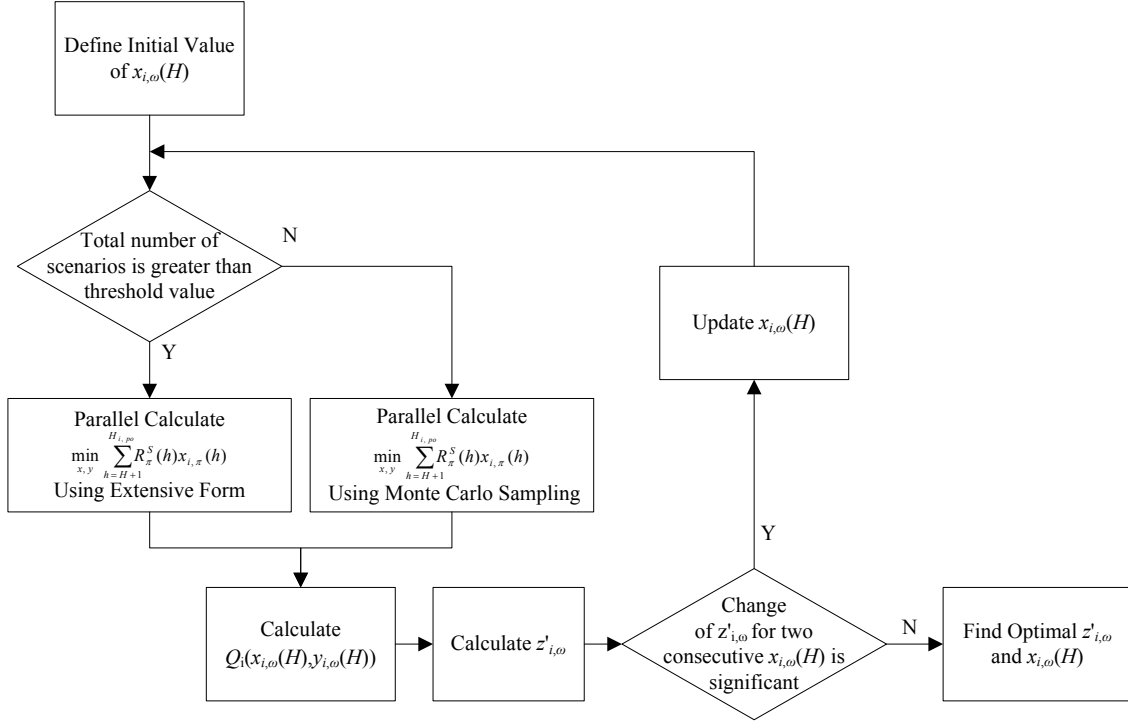
Figure 6 Solution scheme for the proposed solution algorithm

Although it is still impossible to calculate $Q_i(x_{i,\omega}(H), y_{i,\omega}(H))$ with 25^8 scenario within an acceptable time, the proposed PH model enables the implementation of the Monte Carlo sampling method. By applying the Monte Carlo sampling method, the computational burden can be controlled by the user via selecting the appropriate number of samples. Thus, the computational time for solving a scheduling problem with a long plug-in period is controllable.

4.3.5   *Optimality Test of the Proposed Heuristic Solution Method*

A general optimization problem can be described by Eq. (38)-(39).

$$\min f(\mathbf{x}) \tag{38}$$

s.t.

$$\mathbf{g}(\mathbf{x}) \le 0 \tag{39}$$

Without losing generality, by fixing the decision variable x_1 as the parameter, one sub-problem of the above problem can be described by Eq. (40)-(41).

$$\min f(x_2, x_3, \ldots, x_K | x_1) \tag{40}$$

s.t.

$$\mathbf{g}(x_2, x_3, \ldots, x_K | x_1) \le 0 \tag{41}$$

By fixing the rest decision variables as parameter, the counter-part sub-problem can be described by Eq. (42)-(43).

$$\min f(x_1 | x_2, x_3, \ldots, x_K) \tag{42}$$

s.t.

$$\mathbf{g}(x_1 | x_2, x_3, \ldots, x_K) \le 0 \tag{43}$$

By cyclically solving the one sub-problem and use the solution from that sub-problem as the parameters to solve another sub-problem, a final solution denoted as $\mathbf{x}^*$ may be reached when the difference between the current value and its previous value of any element is less than a threshold value defined by the convergence criteria. Obviously, $\mathbf{x}^*$ is a regular point of the original optimization problem.

According to [87-88], if there exists $\lambda^1 \ge 0$, $\lambda^2 \ge 0$, and $\lambda^1 = \lambda^2$ such that

$$\mathbf{J}_1 \nabla^T f(\mathbf{x}^*) + \mathbf{J}_1 \nabla^T \mathbf{g}^1(\mathbf{x}^*) \boldsymbol{\lambda}^1 = 0 \tag{44}$$

$$\left(\mathbf{g}^1(\mathbf{x}^*)\right)^T \boldsymbol{\lambda}^1 = 0 \tag{45}$$

and

$$\mathbf{J}_2 \nabla^T f(\mathbf{x}^*) + \mathbf{J}_2 \nabla^T \mathbf{g}^2(\mathbf{x}^*) \boldsymbol{\lambda}^2 = 0 \tag{46}$$

$$\left(\mathbf{g}^2(\mathbf{x}^*)\right)^T \boldsymbol{\lambda}^2 = 0 \tag{47}$$

where

$$\mathbf{J}_1 = \begin{bmatrix} 1 & 0 & \cdots & 0 \\ 0 & 0 & & \vdots \\ \vdots & & \ddots & \vdots \\ 0 & \cdots & \cdots & 0 \end{bmatrix} \quad \text{and} \quad \mathbf{J}_2 = \begin{bmatrix} 0 & 0 & \cdots & 0 \\ 0 & 1 & & \vdots \\ \vdots & & \ddots & 0 \\ 0 & \cdots & 0 & 1 \end{bmatrix}$$

then $\mathbf{x}^*$ is the optimal solution of the original optimization problem.

Now, in order to prove the optimality of the solution obtained by the proposed solution algorithm, the two-stage stochastic linear program decomposed from the proposed PH model can be written in the extensive form as follows.

$$\begin{aligned} \min z_{i,\omega} &= R_\omega^S(H) x_{i,\omega}^{PH}(H) + Q_i^{PH}\left(x_{i,\omega}^{PH}(H), y_{i,\omega}^{PH}(H)\right) \\ &= R_\omega^S(H) x_{i,\omega}^{PH}(H) + \underset{\pi \in \Pi}{E}\left[\min_{x,y} \sum_{h=H+1}^{H_{i,po}} R_\pi^S(h) x_{i,\pi}^{PH}(h)\right] \\ &= R_\omega^S(H) x_{i,\omega}(H) + \sum_{j=1}^{W} \Pr_{\pi_j} \sum_{h=H+1}^{H_{i,po}} R_{\pi_j}^S(h) x_{i,\pi_j}(h) \qquad \forall i, \omega \end{aligned} \tag{48}$$

s.t.

$$\left(D_{\pi_j}(H)-1\right)x_{i,\omega}(H)+\sum_{h=H+1}^{H_{i,po}}\left(D_{\pi_j}(h)-1\right)x_{i,\pi_j}(h)-A_{\pi_j}\leq 0 \qquad \forall j=1,2,...,W \tag{49}$$

$$-x_{i,\omega}(H)\leq 0 \tag{50}$$

$$x_{i,\omega}(H)-1\leq 0 \tag{51}$$

$$-x_{i,\pi_j}(h)\leq 0 \qquad \forall h=H+1,H+2,...,H_{i,po} \quad \forall j=1,2,...,W \tag{52}$$

$$x_{i,\pi_j}(h)-1\leq 0 \qquad \forall h=H+1,H+2,...,H_{i,po} \quad \forall j=1,2,...,W \tag{53}$$

Then the two sub-problems are formulated as Eq. (54)-(57) and (58)-(61) respectively.

Sub-problem 1:

$$\min z_{i,\omega}^1 = R_\omega^S(H)x_{i,\omega}(H) \qquad \forall i,\omega \tag{54}$$

s.t.

$$\left(D_{\pi_j}(H)-1\right)x_{i,\omega}(H)-A_j^1\leq 0 \qquad \forall j=1,2,...,W \tag{55}$$

$$-x_{i,\omega}(H)\leq 0 \tag{56}$$

$$x_{i,\omega}(H)-1\leq 0 \tag{57}$$

Sub-problem 2:

$$\min z_{i,\omega}^2 = \sum_{j=1}^{W}\mathrm{Pr}_{\pi_j}\sum_{h=H+1}^{H_{i,po}}R_{\pi_j}^S(h)x_{i,\pi_j}(h) \qquad \forall i,\omega \tag{58}$$

s.t.

$$\sum_{h=H+1}^{H_{i,po}}\left(D_{\pi_j}(h)-1\right)x_{i,\pi_j}(h)-A_j^2\leq 0 \qquad \forall j=1,2,...,W \tag{59}$$

$$-x_{i,\pi_j}(h) \le 0 \qquad \forall h = H+1, H+2,..., H_{i,po} \quad \forall j = 1,2,...,W \tag{60}$$

$$x_{i,\pi_j}(h)-1 \le 0 \qquad \forall h = H+1, H+2,..., H_{i,po} \quad \forall j = 1,2,...,W \tag{61}$$

Thus, Eq. (44)-(47) can be written as follows.

$$R_\omega^S(H) + \sum_{j=1}^{W} \lambda_j^1 \left(D_{\pi_j}(H)-1\right) - \lambda_H^{lb} + \lambda_H^{ub} = 0 \tag{62}$$

$$\lambda_j^1 \left\{ \left(D_{\pi_j}(H)-1\right) x_{i,\omega}^*(H) - A_j^1 \right\} = 0 \qquad \forall j = 1,2,...,W \tag{63}$$

$$\lambda_H^{lb} x_{i,\omega}^*(H) = 0 \tag{64}$$

$$\lambda_H^{ub} \left(x_{i,\omega}^*(H)-1\right) = 0 \tag{65}$$

and

$$\sum_{j=1}^{W} \Pr_{\pi_j} \sum_{h=H+1}^{H_{i,po}} R_{\pi_j}^S(h) + \sum_{j=1}^{W} \lambda_j^2 \sum_{h=H+1}^{H_{i,po}} \left(D_{\pi_j}(h)-1\right) - \sum_{j=1}^{W} \sum_{h=H+1}^{H_{i,po}} (\lambda_{h,j}^{lb} - \lambda_{h,j}^{ub}) = 0 \tag{66}$$

$$\lambda_j^2 \left\{ \sum_{h=H+1}^{H_{i,po}} \left(D_{\pi_j}(h)-1\right) x_{i,\pi_j}^*(h) - A_j^2 \right\} = 0 \qquad \forall j = 1,2,...,W \tag{67}$$

$$\lambda_{h,j}^{lb} x_{i,\pi_j}^*(h) = 0 \qquad \forall h = H+1, H+2,..., H_{i,po} \quad \forall j = 1,2,...,W \tag{68}$$

$$\lambda_{h,j}^{ub} \left(x_{i,\pi_j}^*(h)-1\right) = 0 \qquad \forall h = H+1, H+2,..., H_{i,po} \quad \forall j = 1,2,...,W \tag{69}$$

Since λ_H^{lb} and λ_H^{ub} do not appear in Eq. (66)-(69), while $\lambda_{h,j}^{lb}$ and $\lambda_{h,j}^{ub}$ do not appear in the Eq. (62)-(65), the solution is optimal when there exists $\lambda^1 \ge 0$, $\lambda^2 \ge 0$, and $\lambda^1 = \lambda^2$ such that the problem formulated by Eq. (62)-(69) has a non-negative solution.

Because the corresponding elements of $\mathbf{x}^*$ are the optimal solutions of the two sub-problems, for the first sub-problem, there are three situations:

First situation: $x_{i,\omega}^*(H) = 0$ and $\left(D_{\pi_j}(H) - 1\right)x_{i,\omega}^*(H) - A_j^1 \neq 0$ for all j

Second situation: $x_{i,\omega}^*(H) = 0$ and $\left(D_{\pi_j}(H) - 1\right)x_{i,\omega}^*(H) - A_j^1 \neq 0$ not for all j

Third situation: $x_{i,\omega}^*(H) \neq 0$ and $\left(D_{\pi_j}(H) - 1\right)x_{i,\omega}^*(H) - A_j^1 = 0$ for all j

In the first situation, $x_{i,\omega}^*(H) = 0$ means λ_H^{lb} can be any non-negative number and $\lambda_H^{ub} = 0$.

$\left(D_{\pi_j}(H) - 1\right)x_{i,\omega}^*(H) - A_j^1 \neq 0$ means $\boldsymbol{\lambda^1 = \lambda^2 = 0}$, and Eq. (55) and (59) cannot take equality sign.

Thus, $x_{i,\pi_j}^*(h) = 0$, $\lambda_{h,j}^{ub} = 0$ and $\lambda_{h,j}^{lb}$ can be any number. In addition, since the coefficients of

λ_H^{lb} and $\lambda_{h,j}^{lb}$ in Eq. (62) and (66) are negative, their value is positive. Thus, the KKT condition

for the original problem is met and $\mathbf{x}^*$ is the optimal solution of the original problem. The

physical meaning of this situation is that without charging the battery the final SOC when the

vehicle leaves the aggregator is still greater than the desired SOC.

In the second situation, $x_{i,\omega}^*(H) = 0$ means λ_H^{lb} can be any non-negative number and $\lambda_H^{ub} = 0$.

For the j, where $\left(D_{\pi_j}(H) - 1\right)x_{i,\omega}^*(H) - A_j^1 \neq 0$, $\lambda_j^1 = \lambda_j^2 = 0$. Thus, $x_{i,\pi_j}^*(h) = 0$, $\lambda_{h,j}^{ub} = 0$ and $\lambda_{h,j}^{lb}$

can be any number. For the rest of j, where $\left(D_{\pi_j}(H) - 1\right)x_{i,\omega}^*(H) - A_j^1 = 0$, λ_j^1, λ_j^2, $\lambda_{h,j}^{lb}$ and $\lambda_{h,j}^{ub}$

can be any number, and $x_{i,\pi_j}^*(h) \neq 0$ for at least one h. Since the coefficients of λ_j^1, λ_j^2, λ_H^{lb} and

$\lambda_{h,j}^{lb}$ in Eq. (62) and (66) are negative, there exists non-negative solutions, in which $\lambda_j^1 = \lambda_j^2$ for

47

the j where $\left(D_{\pi_j}(H) - 1\right)x^*_{i,\omega}(H) - A^1_j = 0$. Thus, the KKT condition for the original problem is

met and $\mathbf{x}^*$ is the optimal solution of the original problem. The physical meaning of this situation

is that in some scenarios the vehicle needs to be charged so that the final SOC when the vehicle

leaves the aggregator is the desired SOC, while in the rest of scenarios the final SOC when the

vehicle leaves the aggregator is still greater than the desired SOC without charging the battery.

In the third situation, $x^*_{i,\omega}(H) \neq 0$ means, and λ^{ub}_H could any non-negative number.

$\left(D_{\pi_j}(H) - 1\right)x^*_{i,\omega}(H) - A^1_j = 0$ means λ^1_j and λ^2_j can be any number. Since the coefficients of λ^1_j,

λ^2_j in Eq. (62) and (66) are negative, there exists non-negative solutions, where $\lambda^1_j = \lambda^2_j$. Thus,

the KKT condition for the original problem is met and $\mathbf{x}^*$ is the optimal solution of the original

problem. The physical meaning of this situation is that in all scenarios the vehicle needs to be

charged so that the final SOC when the vehicle leaves the aggregator is the desired SOC.

Therefore, the optimality of the proposed heuristic solution method is guaranteed.

4.3.6   *Proposed Fixed-length Time Frame Model*

Another practical way to control the computational burden is not to consider the uncertainty of

stochastic parameters for the entire plug-in period, but only consider in a fix-length time frame.

For example, if the remaining plug-in period of a certain vehicle is eight hours, the parameters

for the first five hours in to the future are considered as stochastic parameters when determining

the charge schedule. The parameters for the last three hours are considered as deterministic

parameters and are estimated by using the predicted mean value. Thus, the total number of

scenario for such a scheduling problem is limited to 25^5. This method can be recognized as

fixed-length time frame method. The corresponding model is formulated as follows and denoted as FT model.

$$z_i = \mathop{E}_{\omega \in \Omega} \left\{ \mathop{\min}_{x,y} R_\omega^S(H) x_{i,\omega}^{FT}(H) + Q_i^{FT}\left(x_{i,\omega}^{FT}(H), y_{i,\omega}^{FT}(H)\right) \right\} \qquad \forall i = 1,2,...,N \tag{70}$$

subject to:

$$y_{i,\omega}^{FT}(H) = \begin{cases} SOC_{i,pi} & H = H_{i,pi} \\ SOC_i(H-1) + \dfrac{P_{max}}{E_{max}}\left(X_i(H-1) + D_\omega(H-1)\left(1 - X_i(H-1)\right)\right) & H_{i,pi} < H \le H_{i,po} \end{cases} \tag{71}$$

$$0 \le x_{i,\omega}^{FT}(H) \le 1 \tag{72}$$

where

$$Q_i^{FT}\left(x_{i,\omega}^{FT}(H), y_{i,\omega}^{FT}(H)\right) = \begin{cases} \mathop{E}_{\pi \in \Pi}\left(\mathop{\min}_{x,y} \sum_{h=H+1}^{H+4} R_\pi^S(h) x_{i,\pi}^{FT}(h) + \sum_{h=H+5}^{H_{i,po}} R_{MV}^S(h) x_{i,\pi}^{FT}(h)\right) & H_{i,po} > H+5 \\ \mathop{E}_{\pi \in \Pi}\left(\mathop{\min}_{x,y} \sum_{h=H+1}^{H_{i,po}} R_\pi^S(h) x_{i,\pi}^{FT}(h)\right) & \text{otherwise} \end{cases} \tag{73}$$

subject to:

$$SOC_{i,tgt} \le y_{i,\omega}^{FT}(H) + \frac{P_{max}}{E_{max}}\left(\begin{matrix} x_{i,\omega}^{FT}(H) + D_\pi(H)\left(1 - x_{i,\omega}^{FT}(H)\right) \\ + \sum_{h=H+1}^{H+4}\left(x_{i,\pi}^{FT}(h) + D_\pi(h)\left(1 - x_{i,\pi}^{FT}(h)\right)\right) \\ + \sum_{h=H+5}^{H_{i,po}} x_{i,\pi}^{FT}(h) \end{matrix} \right) \qquad H_{i,po} > H+5 \tag{74}$$

49

$$SOC_{i,tgt} \leq y_{i,\omega}^{FT}(H) + \frac{P_{max}}{E_{max}} \begin{pmatrix} x_{i,\omega}^{FT}(H) + D_\pi(H)\left(1 - x_{i,\omega}^{FT}(H)\right) \\ + \sum_{h=H+1}^{H_{i,po}} \left(x_{i,\pi}^{FT}(h) + D_\pi(h)\left(1 - x_{i,\pi}^{FT}(h)\right)\right) \end{pmatrix} \qquad H_{i,po} \leq H + 5 \qquad (75)$$

$$0 \leq x_{i,\pi}^{FT}(h) \leq 1 \qquad h = H_{i,pi} + 1, H_{i,pi} + 2, ..., H_{i,po} \qquad (76)$$

The objective function is formulated Eq. (70), which calculates the expected total cost for charging the vehicle and for the failure to provide regulation service from the start of hour H until the EV plugs-out. Eq. (71) determines the SOC of i_{th} EV at the start of hour H under the condition of a possible realization of ω. Eq. (73) calculates the expected cost due to the operation from hour $H+1$ to $H_{i,po}$. Eq. (74) and (75) require that the SOC meets the vehicle owner's need for travel when the vehicle plugs-out. Eq. (72) and (76) define the feasible range of the decision variables.

The reason behind the FT model is that as the prediction time increases, the prediction accuracy will decrease and the risk associated with the decision will also increase. So after certain hours, the improvement of reliability between using the predicted mean value and several scenarios becomes insignificant. Thus, it is not worthwhile to pay a significant extra amount of computational cost for such an insignificant improvement.

On the other hand, the proposed FT model gives the user to control the computational cost, and to study the trade-off between the reliability improvement and the computational cost. Thus, the FT model gives the user the ability to determine the best number of scenarios for each hour into the future, based on the computational resources he has.

4.4 Predictive Frequency Regulation Capacity Bidding for the Aggregator

Generally, the profit of the aggregator for a certain hour based on a given frequency regulation bidding capacity can be expressed as Eq. (77). Since the last term in the last line of Eq. (77) does not contain any decision variables, the maximization of the profit is equivalent to the maximization of the first term.

$$
\begin{aligned}
Profit_{AG}(h) &= \left(R^C(h) + R^P(h)m(h)\right)P(h) - R^E(h)\left(P_{max}n(h) - P(h)\right) - R^E(h)D(h)P(h) \\
&= \left(R^E(h) - R^E(h)D(h) + R^C(h) + R^P(h)m(h)\right)P(h) - R^E(h)P_{max}n(h) \\
&\approx \left(R^E(h) + R^C(h) + R^P(h)M\right)P(h) - R^E(h)P_{max}n(h) \\
&= R^S P(h) - R^E(h)P_{max}n(h)
\end{aligned}
\tag{77}
$$

Therefore, given the optimal operation schedules of each EV obtained from the scheduling model proposed in the previous section, the optimal bidding capacity of the aggregator is determined by the following two-stage stochastic linear program. The proposed stochastic linear program maximizes the revenue of the aggregator by providing frequency regulation service in the hour H.

$$
\max_{p} z = \mathop{E}_{\omega \in \Omega}\left\{R_\omega^S(H)p(H) - R_\omega^{S+}(H)\max\left(p(H) - P_\omega^A(H), 0\right) - R_\omega^{S-}(H)\max\left(P_\omega^A(H) - p(H), 0\right)\right\}
\tag{78}
$$

subject to

$$
0 \leq p(H) \leq P_{max}n(H)
\tag{79}
$$

where

$$
P_\omega^A(H) = \sum_{i=1}^{n(H)}\left(1 - x^*_{i,\omega}(H)\right) \qquad \forall \omega \in \Omega
\tag{80}
$$

The first term in the objective function, which is Eq. (78), stands for the profit of the aggregator for frequency regulation. The second and third terms derive the penalty cost when the aggregated frequency regulation capacity, P^A_ω, is different from the bidding capacity, p. Eq. (79) requires that the proposed frequency regulation bidding capacity should not be greater than the maximum total power from all available vehicles.

It is important to note that the aggregated frequency regulation capacity, P^A_ω, is determined by the optimal schedules obtained from the scheduling model for individual vehicles according to Eq. (80). Since the optimal schedule is a stochastic parameter with respect to ω, P^A_ω is also stochastic. This indicates that a possible realization of P^A_ω could be either higher or lower than the bidding capacity, p.

However, the operation is executed based on the smaller of the two in real world operation. In other words, if $p > P^A_\omega$, the operation will be based on P^A_ω, because the aggregator cannot provide more capacity than what is available. On the contrary, the operation will be based on p, because providing more capacity than what is settled in the contract will not be credited.

Obviously, the mismatch between P^A_ω and p may result in a loss of profit. When $p < P^A_\omega$, the aggregator is losing money because of 1) its failure to fully utilize the available capacity and 2) a higher charging point than necessary at a relatively higher rate. In contrast, when $p > P^A_\omega$, the aggregator needs to buy the shortage of frequency regulation capacity from other regulators at a potentially higher rate to meet the contract.

In practice, R^+_ω and R^-_ω rely on R^S_ω, and should be no smaller than R^S_ω. Moreover, there is a correlation between parameters R^+_ω, R^-_ω and R^S_ω. However, there is also a special case when R^+_ω

and R^-_ω are identical to R^S_ω. In this case, the optimal bidding capacity of the aggregator is the maximum of all possible P^A_ω.

After obtaining the optimal bidding frequency regulation power capacity of the aggregator for hour H, namely $p^*(H)$, the corresponding coordinated operation schedules of individual EVs for the same hour, namely $X_{i,\omega}(H)$, can be calculated by using the following equation.

$$X_{i,\omega}(H) = \begin{cases} x^*_{i,\omega}(H) & p^*(H) \geq P^A_\omega(H) \\ 1-\left(1-x^*_{i,\omega}(H)\right)p^*(H)\big/P^A_\omega(H) & otherwise \end{cases} \tag{81}$$

Basically, if $p > P^A_\omega$, vehicles will keep their original schedule. However, if $p < P^A_\omega$, the shortage between p and P^A_ω will be evenly distributed to each vehicle. Correspondingly, adjustments are made to their schedules. The finalized schedule, X_ω, will be used to determine the operation schedule of each vehicle and the capacity bidding of the aggregator for hour $H+1$.

4.5 Real-time Synergetic Dispatch

Suppose the aggregator receives a new regulation signal from the grid operator at the start of that arbitrary time interval t. To maintain the SOC of the vehicles in $\mathbf{S}^+$ is within the normal range, which is between $SOC_{min}+SOC_{rsv}$ and $SOC_{max}-SOC_{rsv}$, d^+_{adj} should be as large as possible. This ensures that the adjusted regulation signal for those vehicles, $d(t)-d^+_{adj}$, will be as small as possible. Correspondingly, for the vehicles in $\mathbf{S}^-$, d^-_{adj} should also be as large as possible, so that the adjusted regulation signal for those vehicles, $d(t)+d^-_{adj}$, can be as large as possible. The vehicles in $\mathbf{S}$ should evenly share the total adjustment to the regulation signals from vehicles in those two sets.

Thus, the real-time dispatch model can be formulated as a linear program, where the objective function is to maximize the adjustment to the regulation signal for each vehicle in $\mathbf{S}^-$ and $\mathbf{S}^+$. Hence, the optimal adjustments to the regulation signal for all the vehicles are generated by solving the following problem.

$$\max_{d_{adj}, d_{adj}^+, d_{adj}^-} \quad z = d_{adj}^+(t) + d_{adj}^-(t) \qquad \forall t \in h \tag{82}$$

subject to:

$$\sum_{i \in \mathbf{S}(t)} \left(1 - X_i(h)\right) d_{adj}(t) = \sum_{i \in \mathbf{S}^+(t)} \left(1 - X_i(h)\right) d_{adj}^+(t) - \sum_{i \in \mathbf{S}^-(t)} \left(1 - X_i(h)\right) d_{adj}^-(t) \tag{83}$$

$$-1 \le d(t) + d_{adj}(t) \le 1 \tag{84}$$

$$d(t) - d_{adj}^+(t) \ge -1 \tag{85}$$

$$d(t) + d_{adj}^-(t) \le 1 \tag{86}$$

$$d_{adj}^+(t), d_{adj}^-(t) \ge 0 \tag{87}$$

The objective function maximizes the adjustment to the original frequency regulation signal for all vehicles in $\mathbf{S}^-$ and $\mathbf{S}^+$. There are three constraints in the dispatch model. The adjustment to the regulation signals for vehicles in $\mathbf{S}$ is calculated by using Eq. (83). Equation (84) ensures that the adjusted regulation signals for the vehicles in $\mathbf{S}$ is within the range of -1 and 1, after evenly sharing the total adjustment to regulation signal from vehicles in the other two sets. Equations (85) and (86) require that the adjusted regulation signals for the vehicles in $\mathbf{S}^+$ and $\mathbf{S}^-$ also fall within the range of -1 and 1. However, because $d(t)$ is between -1 and 1 and d^+_{adj} is non-negative, $d(t)$-d^+_{adj} is always less than 1. Similarly, $d(t)$+ d^-_{adj} is always greater than -1. Therefore, only one

side of the boundary needs to be considered. Eq. (84) defines the feasible region of the decision variables

Then, the final actual charge or discharge signal for each vehicle at time t is calculated as follows.

$$d_{i,act}(t) = \begin{cases} X_i(h) + (1 - X_i(h))\left(d(t) - d_{adj}^{+*}(t)\right) & i \in \mathbf{S}^+(t) \\ X_i(h) + (1 - X_i(h))\left(d(t) + d_{adj}^{-*}(t)\right) & i \in \mathbf{S}^-(t) \\ X_i(h) + (1 - X_i(h))\left(d(t) + d_{adj}^{*}(t)\right) & i \in \mathbf{S}(t) \end{cases} \tag{88}$$

Depending on the value of $d_{i,act}(t)$, vehicles in $\mathbf{S}^+$ can generally have two different actions. If $d_{i,act}(t)$ is negative, the vehicles in $\mathbf{S}^+$ are in the active discharging process, and the SOC of those vehicles will be gradually reduced to SOC_{max}-SOC_{rsv} or below. According to Figure 2, there is a very rare chance that the regulation signal consistently reaches 1 for a long period of time. Therefore, it is very likely that the SOC of the EVs in $\mathbf{S}^+$ can be reduced by actively discharging the battery. Hence, through the proper assignment of the charge or discharge signal to each EV, the SOC of each EV can be maintained at a safe level between SOC_{min} and SOC_{max}. For example, assume there are three EVs and their SOCs are 0.5, 0.6 and 1.0 respectively. The new regulation signal is 0.6. Instead of assigning a signal of 0.6 to each EV, which is infeasible because the third vehicle would be over-charged, the aggregator could assign 1.0 to the first two EVs and -0.2 to the last EV. If $d_{i,act}(t)$ is positive, the vehicles in S+ are in the forced charging process and the SOCs of those vehicles are still rising. In this situation, SOC_{rsv} is necessary to buffer the forced charged energy so that the battery will not be over-charged. In the same way, vehicles in $\mathbf{S}^-$ can also be in two similar processes. If $d_{i,act}(t)$ is negative, the vehicles in $\mathbf{S}^-$ are in the forced discharging process; and vice versa.

Although the proposed real-time synergetic dispatch model requires additional computational efforts for the aggregator, such additional computational efforts are not significant. Based on the proposed model, the signal adjustment occurs only when there are vehicles in either $\mathbf{S}^-$ or $\mathbf{S}^+$. However, for most of the time the SOCs of vehicles are between $SOC_{\min}+SOC_{rsv}$ and $SOC_{\max}-SOC_{rsv}$. Thus, vehicles are all in $\mathbf{S}$ and no vehicles are in $\mathbf{S}^-$ or $\mathbf{S}^+$ during the majority of the time, and no signal adjustments are needed. Therefore, the signal adjustment is infrequent and the computational efforts required for that are limited and minor.

When the regulation signal adjustment occurs, vehicles in $\mathbf{S}^-$ and $\mathbf{S}^+$ are actually using the capacity of vehicles in $\mathbf{S}$ to meet the frequency regulation service obligation. Thus, the part of profit earned by vehicles in $\mathbf{S}^-$ and $\mathbf{S}^+$ during that time should be literally credited to the vehicles in $\mathbf{S}$. However, the proper assignment of that part of profit is straightforward and therefore is not discussed in this thesis.

Considering the possible lag in communication between the aggregator and individual EVs, the information of a vehicle's status may not be available immediately at the start of time interval t, when a new regulation signal arrives. Thus, instead of using the information of a vehicle's status at time t, the most recent available information, such as at time t-1 or t-2, could be used. Moreover, the disptach model can use the regulation signal predicted by time series models.

It is also necessary to note that the determination of SOC_{rsv} is important, because it may affect both the battery charge schedule and final battery SOC. Generally, a higher value of SOC_{rsv} means that the regulation signal adjustment is more likely to occur, but the battery is less likely to be over-charged. However, for vehicles whose SOC_{drv} is equal to $SOC_{\max}-SOC_{\min}$, a higher

value of SOC_{rsv} means lower $SOC_{i,tgt}$ based on Eq. (34). As a result, this leads to higher inconvenience for the vehicle owner, less charging time and a higher profit for the vehicle. Nevertheless, such a high value of SOC_{rsv} will not affect the majority of vehicle owners based on [84].

The optimal value of SOC_{rsv} should be determined based on the driving profile of EVs and the regulation signal profile. The optimal value can be determined through the simulation of the charging process based on historical data. The lowest SOC_{rsv} that ensures no frequency regulation capacity reduction and battery over-charge is the optimal value.

CHAPTER 5

SIMULATION RESULT

This chapter presents the simulation results by using the proposed PH and FT models on an arbitrary aggregator for an office building garage from May 1 to May 10 2014. The results are compared with those obtained by using the PI, the MV, the YM and the HN models. An additional simulation is conducted to investigate the performance of the proposed synergetic dispatch model for different settings for the period of June 1, 2013 to May 31, 2014.

5.1   Introduction of simulation background

There are 100 participating EVs in both simulations, while each EV has a battery capacity of 24 kWh. The maximum charge and discharge rates of the battery are 0.15C, or equivalently 3.6 kW for both directions.
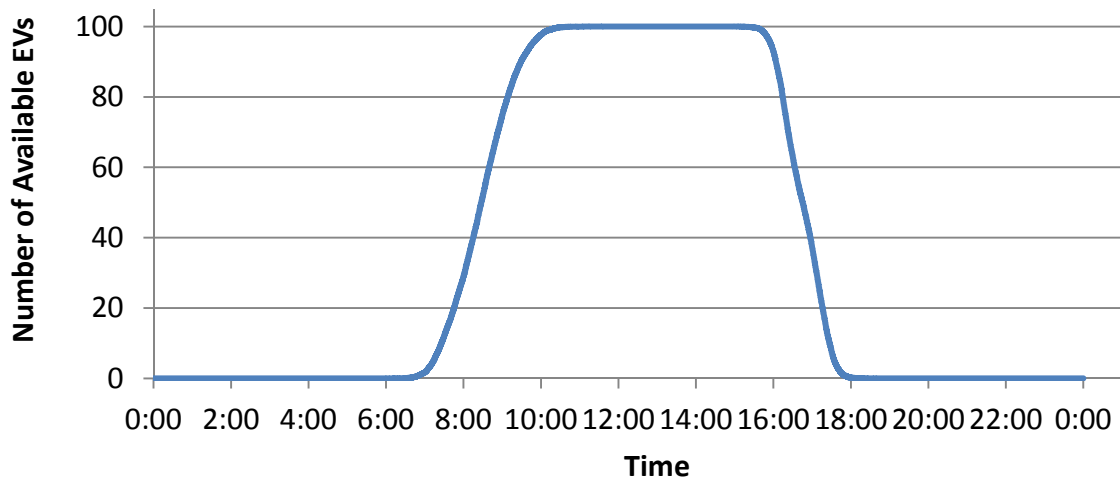
Figure 7 Profile of total number of available EVs in a day

In the first simulation, $SOC_{\min}$, $SOC_{\max}$ and SOC_{rsv} are assumed to be 0, 1 and 0.025 respectively. The availability profit of each EV is generated randomly and illustrated by Figure 7. $SOC_{i,\mathrm{drv}}$ is generated based on the driving profile reported in [84] and shown in Figure 8. The real-time frequency regulation credit rate, real-time energy rate and real-time frequency regulation signal are obtained from PJM website [82, 85-86]. The simulation is performed by using Matlab® R2016a on a PC with Intel® Core i7-4770, 16 Gb RAM and NVIDIA GeForce® GT 730 graphic card.
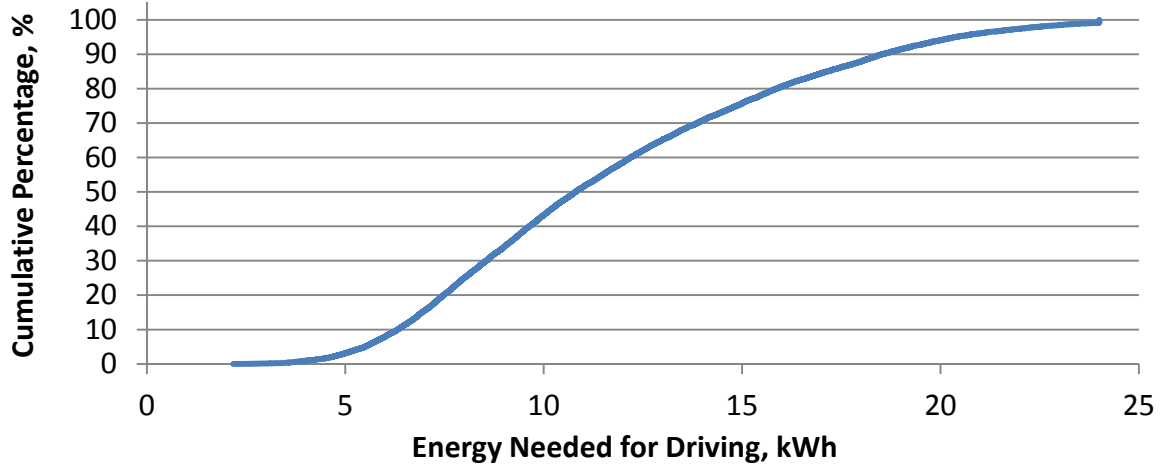
Figure 8 Profile of energy needed for driving

5.2   Electricity Market Prices Prediction

An accurate prediction of the actual aggregated rate (R^S) is important for the operation of electricity generation units and electricity consumers. However, the development of a new prediction model is beyond the scope of this thesis. Therefore, a seasonal autoregressive model is directly implemented in the simulation. The best fit model is expressed as Eq. (89).

$$R^S(h) = 0.622613\ R^S(h-1) + 0.1347219\ R^S(h-2) + 0.062033\ R^S(h-3) + 0.186\ R^S(h-24)$$

$$(89)$$
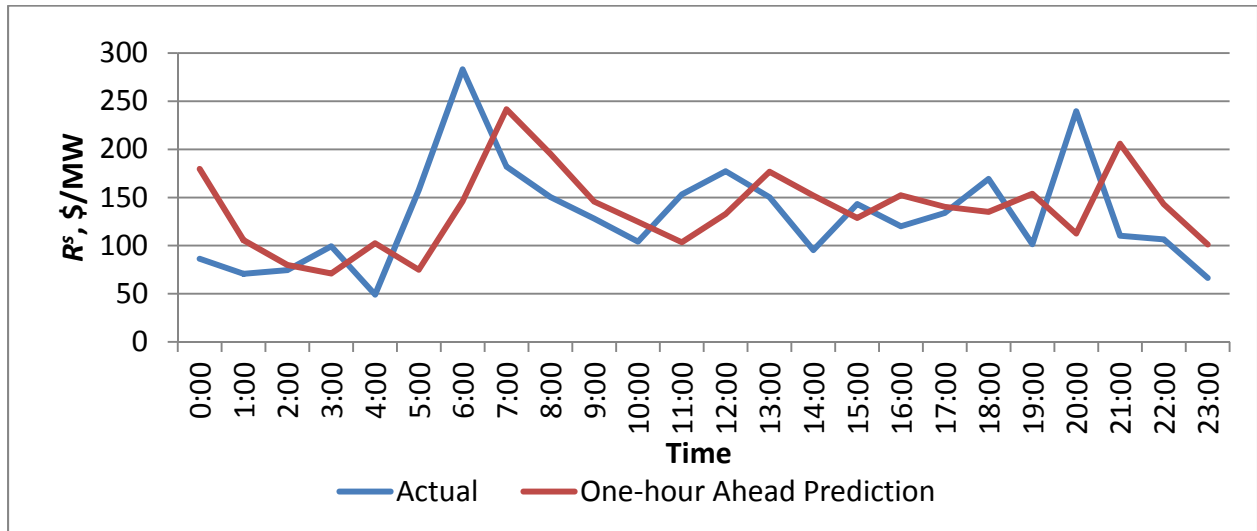
Figure 9 Actual and one-hour ahead predicted R^S for May 1st 2014
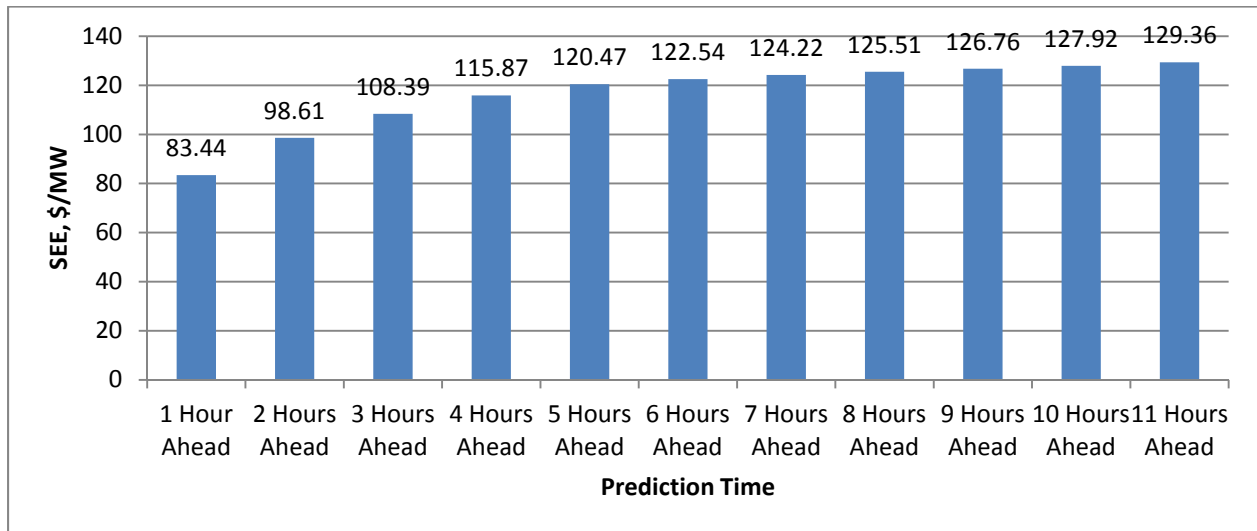
Figure 10 Prediction error of aggregated cost rate with different prediction time

The actual and one-hour ahead prediction of R^s obtained using the model for May 1st 2014 is illustrated by Figure 9, while the standard error of estimate (SEE) for different prediction times are compared in Figure 10.

5.3   Scenario Description

Generally, the actual aggregated cost rate can be decomposed into its prediction mean and prediction error. The actual aggregated cost rate is one of the important stochastic parameters that are considered when making schedules using the proposed model. Since the prediction mean for a specific hour is a deterministic parameter, the consideration of the actual aggregated cost rate is equivalent to the consideration of its prediction error when making a schedule. Since the optimality of the scenario is beyond the scope of this thesis, five scenarios are generated for the two stochastic parameters considered in the model: predicted aggregated rate and hourly average regulation signal. Details of the scenarios are listed in Tables 1 and 2.

Table 1 Scenarios of Prediction Error of Aggregated Cost Rate

Prediction time	Scenario	Value	Range	Probability
1 Hour Ahead	1	-102.77	(-∞, -56.19)	0.125
	2	-35.56	[-56.19, -21.08)	0.225
	3	-6.78	[-21.08, 9.24)	0.300
	4	28.95	[9.24, 56.13)	0.225
	5	131.10	[56.13, ∞)	0.125
2 Hours Ahead	1	-114.27	(-∞, -66.23)	0.125
	2	-42.83	[-66.23, -25.81)	0.225
	3	-8.44	[-25.81, 10.56)	0.300
	4	32.69	[10.56, 63.48)	0.225
	5	153.02	[63.48, ∞)	0.125
3 Hours Ahead	1	-119.24	(-∞, -73.10)	0.125
	2	-48.06	[-73.10, -29.52)	0.225
	3	-9.89	[-29.52, 12.09)	0.300
	4	35.61	[12.09, 67.94)	0.225
	5	165.74	[67.94, ∞)	0.125
4 Hours Ahead	1	-121.83	(-∞, -76.32)	0.125
	2	-51.85	[-76.32, -32.52)	0.225
	3	-11.20	[-32.52, 11.94)	0.300
	4	36.38	[11.94, 71.18)	0.225
	5	177.00	[71.18, ∞)	0.125

Table 2 Scenarios of Prediction Error of Aggregated Cost Rate (Continued)

Prediction time	Scenario	Value	Range	Probability
5 Hours Ahead	1	-123.50	(-∞, -77.43)	0.125
	2	-53.61	[-77.43, -34.23)	0.225
	3	-12.00	[-34.23, 11.86)	0.300
	4	36.62	[11.86, 71.52)	0.225
	5	183.39	[71.52, ∞)	0.125
6 Hours Ahead	1	-121.60	(-∞, -78.33)	0.125
	2	-54.76	[-78.33, -25.66)	0.225
	3	-13.43	[-25.66, 10.12)	0.300
	4	36.48	[10.12, 73.04)	0.225
	5	187.28	[73.04, ∞)	0.125
7 Hours Ahead	1	-120.15	(-∞, -78.30)	0.125
	2	-55.16	[-78.30, -37.16)	0.225
	3	-14.24	[-37.16, 9.59)	0.300
	4	35.50	[9.59, 71.76)	0.225
	5	190.34	[71.76, ∞)	0.125
8 Hours Ahead	1	-118.48	(-∞, -77.55)	0.125
	2	-56.10	[-77.55, -38.30)	0.225
	3	-15.10	[-38.30, 8.91)	0.300
	4	35.04	[8.91, 71.26)	0.225
	5	193.31	[71.26, ∞)	0.125
9 Hours Ahead	1	-117.47	(-∞, -77.38)	0.125
	2	-56.72	[-77.38, -38.91)	0.225
	3	-15.88	[-38.91, 8.42)	0.300
	4	34.38	[8.42, 71.03)	0.225
	5	196.50	[71.03, ∞)	0.125
10 Hours Ahead	1	-116.74	(-∞, -77.64)	0.125
	2	-57.26	[-77.64, -39.78)	0.225
	3	-16.61	[-39.78, 8.22)	0.300
	4	34.10	[8.22,70.53)	0.225
	5	199.05	[70.53, ∞)	0.125
11 Hours Ahead	1	-116.83	(-∞, -77.45)	0.125
	2	-57.47	[-77.45, -39.78)	0.225
	3	-17.06	[-39.78, 6.99)	0.300
	4	33.46	[6.99, 70.76)	0.225
	5	201.78	[70.76, ∞)	0.125

Table 2 Scenarios of Hourly Average Regulation Signal

Scenario	Value	Range	Probability
1	-0.6953	[-1, -0.4740)	0.125
2	-0.3063	[-0.4740, -0.1777)	0.225
3	-0.0536	[-0.1777, 0.0691)	0.300
4	0.1813	[0.0691, 0.3234)	0.225
5	0.5188	[0.3234, 1]	0.125

5.4 Operation Simulation

In the first simulation, the extensive form of the proposed scheduling model for individual vehicles is used to determine the schedule of an individual vehicle when its remaining plug-in period is seven hours or less. The total number of scenarios is $5^{13} \approx 1.22 \times 10^9$ when the remaining plug-in period is seven hours. On the contrary, Monte Carlo sampling is used to determine the schedule of an individual vehicle when its remaining plug-in period is eight hours or more. 5^{11} samples are generated for the third stage of the proposed model. Therefore, the total number of scenarios is still $5^{13} \approx 1.22 \times 10^9$ in this case. It is important to note that those two numbers become $5^{12} = 2.44 \times 10^8$ when the target hour is the first whole hour after plug-in. Without explicit specification, the following discussion considers situations in which the target hour is not the first hour after an individual vehicle plug-in.

Table 3 compares the running times to finish the calculation which determines the schedule of an individual vehicle with different remaining plug-in periods for the 100 EVs by using three different models. Generally, the running time increases as the remaining plug-in hours increase. The PH model requires significantly higher computational time than the FT model when the remaining plug-in hours is greater than 7. As for the HN model, the running times for the cases where the remaining plug-in hours are greater than 6 are not available, because the calculation of

those cases requires more than 16 Gb of memory and therefore the computation cannot be completed by the desktop. However, when the remaining plug-in hours are less than 5, the HN model requires significantly higher time and memory than the PH and FT models. For example, when the remaining plug-in hours are 5, the HN model requires 5 Gb of memory. On the contrary, the PH and FT models require about 4Gb and 12 Gb of memory when the remaining plug-in hours are 5 and 10 respectively. Therefore, the proposed PH and FT models significantly reduce the computational efforts.

Table 3 Running Time with Different Remaining Plug-in Periods for a Single Vehicle

		Running Time, minutes						
		PH Model			FT Model			HN Model
		Minimum	Average	Maximum	Minimum	Average	Maximum	
Remaining Plug-in Hours	10	211.67	218.73	229.08	7.36	7.58	7.97	NA
	9	35.27	159.83	212.98	1.24	5.69	7.26	NA
	8	30.56	141.39	175.02	1.11	5.14	6.65	NA
	7	22.34	108.95	140.97	0.97	4.71	5.82	NA
	6	0.75	3.66	4.69	0.75	3.72	4.70	67.16
	5	0.03	0.16	0.22	0.04	0.17	0.24	2.92
	4	<0.01	0.02	0.02	<0.01	0.02	0.03	0.14
	3	<0.01	<0.01	<0.01	<0.01	<0.01	<0.01	0.03
	2	<0.01	<0.01	<0.01	<0.01	<0.01	<0.01	0.03

Table 4 presents the total running times to complete the calculation which determines the schedule of all 100 vehicles for a specific hour. The total running times to complete the calculation on two types of graphic card are also compared in Table 4. Basically, the total running time increases from 8:00 to 11:00 as more and more vehicles plug-in, while it decreases after 11:00 as the average remaining plug-in period decreases. The heaviest computational burden occurs when determining the schedule for 11:00.

Table 4 Total Running to Determine the Schedule of 100 Vehicles for a Specific Hour

	Hour of the Day	Number of Available Vehicles	PH Model		FT Model	
			GT 730	GTX 1050 TI	GT 730	GTX 1050 TI
Running Time, hours	8:00	25	10.1	2.74	0.32	0.09
	9:00	69	68.5	17.18	2.33	0.68
	10:00	98	155.8	41.28	5.65	1.70
	11:00	100	176.4	52.06	6.99	2.18
	12:00	100	80.2	25.62	5.81	1.81
	13:00	100	2.71	1.62	2.45	0.75
	14:00	100	0.10	0.11	0.12	0.05
	15:00	100	0.01	0.03	0.02	0.01
	16:00	91	<0.01	0.01	<0.01	<0.01
	17:00	39	<0.01	<0.01	<0.01	<0.01

As it is shown in the table, it takes significant amount of time to finish the computation for the schedule at 11:00, which is not acceptable for real-world implementation. However, such effort could be reduced without using a super computer. Compared with NVIDIA GeForce® GT 730 which has 384 cores in total with 902 MHz for each core, NVIDIA GeForce® GTX 1050 TI has 768 cares in total with 1392 MHz for each core. Theoretically, the total running time for by using NVIDIA GeForce® GT 730 should be 3.0865 times longer than that of using NVIDIA GeForce® GTX 1050 TI. As a matter of fact, the actual rate is higher than 3.10 based on the results shown in Table 4. Hence, if a NVIDIA GeForce® GTX 1080 TI graphic card is used, which has 3584 cores altogether with 1556 MHz for each core, theoretically the total running time can be reduce by 93.79%, comparing to NVIDIA GeForce® GT 730. Thus, the total running time for 11:00 can be reduced to 11.0 hours and 0.434 hours by using the PH and the FT models respectively. If 4 NVIDIA GeForce® GTX 1080 TI graphic cards are used in parallel, the total running time through the PH model can be further reduced to 0.683 hours, while

through the FT model it can be reduced to 0.1085 hours, which is about 6.5 minutes. Therefore, the computational burden is within an acceptable range with acceptable computational cost.

Table 5 lists the optimal expected operational cost calculated at different time point by using the PH, the FT, the HN and the MV models for two vehicles that are randomly selected. Basically, the optimal expected operational cost obtained by the PH model is lower than that obtained by using the FT model when the planning period is longer than 5 hours. When the planning period is less than 5 hours, the optimal expected operational costs obtained by the two models are the same, because they have the same formulation in this situation.

Table 5 Optimal Expected Operational Cost Obtained by Using Different Methods

		Cost, $							
Vehicle No.		1				2			
Model		PH	FT	HN	MV	PH	FT	HN	MV
Hour of the Day	9:00	-	-	-	-	0.25	0.30	NA	0.49
	10:00	-	-	-	-	0.38	0.40	NA	0.59
	11:00	1.15	1.29	NA	1.65	0.25	0.25	NA	0.79
	12:00	0.89	0.95	NA	1.85	0.24	0.24	0.25	0.27
	13:00	0.56	0.56	NA	1.70	0.24	0.24	0.26	0.28
	14:00	0.53	0.53	0.73	0.87	0.29	0.29	0.30	0.31
	15:00	0.44	0.44	0.60	1.06	0.21	0.21	0.21	0.42
	16:00	0.23	0.23	0.34	0.89	-	-	-	-
	17:00	0.13	0.13	0.13	0.34	-	-	-	-

In contrast, the optimal expected operational cost obtained by the HN model is greater than those of the PH and FT models, because as mentioned in the previous discussion the HN model is more conservative. In addition, the optimal expected operational cost obtained by the MV model is always highest among the four models. It is also important to note that the optimal operational cost does not constantly decrease as the time approaches the vehicle's plug-out time. This is due

to the variation of cost rate prediction. As mentioned in a previous section, the predictions of the

cost rate generated at two adjacent hours are always different. Therefore, the optimal expected

operational cost from a later hour could be higher than a previous hour in practice, due to a

sudden spike in the predicted cost rates.

Table 6 Comparison of Vehicle's Operational Cost

		Operational Cost, $							
Vehicle No.		1				2			
Method		PH	FT	MV	PI	PH	FT	MV	PI
Hour of the Day	9:00	-	-	-	-	0.000	0.092	0.271	0.271
	10:00	-	-	-	-	0.170	0.112	0.000	0.000
	11:00	0.301	0.471	0.475	0.000	0.000	0.000	0.135	0.000
	12:00	0.346	0.346	0.346	0.242	0.000	0.000	0.096	0.000
	13:00	0.069	0.000	0.260	0.000	0.000	0.000	0.000	0.000
	14:00	0.237	0.185	0.280	0.000	0.247	0.205	0.000	0.000
	15:00	0.208	0.202	0.268	0.268	0.144	0.135	0.000	0.083
	16:00	0.113	0.108	0.084	0.270	-	-	-	-
	17:00	0.153	0.153	0.000	0.313	-	-	-	-
Total Cost, $		1.426	1.465	1.712	1.092	0.561	0.544	0.502	0.355
Total Profit, $		1.029	0.991	0.743	1.363	1.468	1.485	1.527	1.674
Cost of Prefect Information, $		0.334	0.373	0.620	-	0.206	0.189	0.147	-

The operational costs for May 1 2014 by using the different models are compared in Table 6.

Since the solution of HN model cannot be obtained within a reasonable time, the result of HN

model is not compared in Tables 6. Basically, the operations based on the schedule generated by

using the PH and the FT models are similar but considerably different from the operation

obtained based on the MV and PI models. Since both the cost rate and the hourly average

frequency regulation signal for future hours are uncertain when making the schedule, the

proposed PH and FT models tend to avoid high operational cost by spreading the charging need

to the hours with relatively low aggregated cost rate according to the predicted prices. In addition,

different Table 5, the daily operational cost obtained by using the MV model could be higher than that obtained by using the PH and FT models, due to such uncertainty.

Table 7 lists the operational cost, profit and cost of prefect information of 100 vehicles for 10 days' operation. Generally, the total operational profits obtained by using the PH and FT models for 10 days are $1393.32 and $1409.42 respectively. The similar profits suggest that the consideration of the stochastic parameters after five hours from the target hour does not guarantee a more profitable schedule. In other words, those stochastic parameters are not as valuable as those within five hours from the target hour. Thus, PH model is not significantly better than FT model. However, the fact that FT model requires less computational time makes it a more suitable model for practical implementation.

Meanwhile, the profits by using the PH and FT models are about 20.32% and 21.71% higher than that obtained by using the MV model, while they are about 10.47% and 9.43% lower than that obtained by using the PI model. Thus, the information cost can be reduced on an average of 59.09% and 63.14%, by using the PH and the FT models, when compared with the MV model.

Although the YM model may have a higher profit in some days than the other three models, the low prediction accuracy by directly using yesterday's market day suggests unreliable performance. Therefore, statistically it can make less profit than the other three models.

Table 7 Comparison of 100 Vehicles' Daily Operational Cost

	Model	Operational Profit, $					Cost of Prefect Information, $			
		PH	FT	MV	YM	PI	PH	FT	MV	YM
Day of the Month	1	176.26	176.59	166.53	173.70	190.74	14.48	14.15	24.21	17.05
	2	120.62	119.47	84.46	94.44	126.84	6.22	7.37	42.38	32.40
	3	187.45	192.71	151.30	157.28	197.65	10.19	4.94	46.34	40.37
	4	242.59	241.59	229.43	246.42	262.96	20.38	21.37	33.93	16.54
	5	49.06	54.13	38.72	5.99	69.82	20.76	15.69	31.10	63.82
	6	120.87	123.54	91.73	104.58	140.51	19.64	16.97	48.78	35.93
	7	120.62	120.14	113.54	104.94	140.92	20.30	20.78	27.38	35.99
	8	173.34	171.50	145.78	110.59	205.33	31.99	33.82	59.55	94.74
	9	65.81	72.58	37.30	22.60	78.64	12.84	6.07	41.34	56.04
	10	136.70	137.18	99.54	102.90	142.77	6.07	5.59	43.23	39.87
Total, $		1393	1409	1158	1123	1556	162.86	146.76	398.15	432.74

69

Table 8 lists the optimal frequency regulation bidding capacities based on the proposed PH and the PI models. Because the determination of the optimal frequency regulation bidding capacity is based on all individual vehicles' schedules according to the proposed algorithm, the aggregator's operation also tries to avoid the risk of high operation cost. Because both R^+ and R^- are identical to R^S in the simulation, the optimal frequency regulation bidding capacity equal to product of the number of plug-in vehicles, $n(h)$, and the maximum power of a single EV, P_{max}.

Table 8 Bidding Capacity of the Aggregator for Each Hour

Hour of the Day	Bidding Capacity, kW									
	8:00	9:00	10:00	11:00	12:00	13:00	14:00	15:00	16:00	17:00
PH Method	90.0	248.4	352.8	360.0	360.0	360.0	360.0	356.4	327.6	140.4
FT Method	90.0	248.4	352.8	360.0	360.0	360.0	360.0	356.4	327.6	140.4
MV Method	90.0	100.5	352.8	179.8	180.5	310.1	309.0	275.4	279.9	138.9
PI Method	90.0	98.5	272.9	360.0	318.7	345.2	357.5	176.6	203.4	115.7

Table 9 presents the number of full discharge circles for 100 vehicles for different days by using different models. Theoretically, the number of full discharge circles increases as the total frequency regulation power capacity increases. A higher total frequency regulation power capacity means a higher profit. Therefore, the number of full discharge circles by using the PI method is in generally higher than those of the other three models, because the PI model has the highest profit. On the contrary, the number of full discharge circles by using the MV model is the lowest in general, as the MV model has the lowest profit. On average, V2G frequency regulation contributes 0.11 full discharge circles to one vehicle's battery, which is significantly lower than

what is contributed by daily travel for most vehicles. Based on [8], that will cost each vehicle approximately $0.15 dollars per day. Therefore, the battery degradation due to frequency regulation is not significant and the cost for the degradation can be covered by the profit earned from providing frequency regulation service.

Table 9 Number of Full Discharge Circles

Model		Day of the Month										Total
		1	2	3	4	5	6	7	8	9	10	
Full Discharge Circles	PH	8.32	11.08	10.80	10.19	13.19	12.41	10.41	11.26	12.46	13.47	114
	FT	8.25	11.00	10.72	10.10	12.75	12.44	10.03	11.13	12.43	13.51	112
	MV	9.72	9.88	10.19	9.94	11.08	11.01	12.00	10.96	10.96	11.94	108
	PI	10.62	11.31	10.70	11.04	12.40	12.71	12.74	11.22	11.72	12.87	117

5.5   Real-time Dispatch Simulation

Due to the 100 vehicles' driving profiles, there is no adjustment of frequency regulation signal in the aforementioned simulation. Therefore, in order to investigate the performance of the real-time synergetic dispatch model, another simulation is conducted. The new simulation is performed on 100 vehicles for each hour from June 1st 2013 to May 31st 2014. That is 8760 hours in total. Specific numbers of vehicles are assigned to S^+ at the start of each hour, while the rest of the vehicles are assigned to S. To be specific, among the 100 vehicles, the number of vehicles in S^+ is N_p. In addition, those vehicles in S^+ have an SOC of SOC_{max}-SOC_{rsv} at the start of each hour, while the rest of the vehicles have an SOC of 0.5. Different values of SOC_{rsv} are

used in this simulation to assess the success rate of the operation of each hour. If the SOC of any

vehicle does not exceed SOC_{max} during a certain hour, it is called a success.

The simulation results are presented in Table 10. Generally, as N_p increases, fewer successes are

achieved. On the contrary, the higher SOC_{rsv}, the higher number of successes are realized. Based

on Figure 8, about 5% of vehicles have a SOC_{drv} of more than 0.95. Only those vehicles may

need frequency regulation signal. Therefore, 0.040 is the optimal SOC_{rsv}. For real world

operation, 0.020 is an economical value, because the failure rate is less than 0.15% when N_p is no

greater than 20.

Table 10 Success Rate for Different Parameters

		Success Rate, %									
	N_p	5	10	15	20	25	30	35	40	45	50
SOC_{rsv}	0.005	96.1	95.7	95.2	94.7	94.2	93.5	92.9	92.4	91.6	90.7
	0.010	99.1	98.9	98.9	98.8	98.7	98.7	98.5	98.2	98.1	97.8
	0.015	99.7	99.7	99.6	99.6	99.5	99.4	99.4	99.3	99.3	99.2
	0.020	99.9	99.9	99.9	99.9	99.9	99.9	99.9	99.8	99.8	99.8
	0.025	100.0	100.0	100.0	100.0	100.0	100.0	100.0	99.99	99.9	99.9
	0.030	100.0	100.0	100.0	100.0	100.0	100.0	100.0	100.0	100.0	100.0
	0.035	100.0	100.0	100.0	100.0	100.0	100.0	100.0	100.0	100.0	100.0
	0.040	100.0	100.0	100.0	100.0	100.0	100.0	100.0	100.0	100.0	100.0
	0.045	100.0	100.0	100.0	100.0	100.0	100.0	100.0	100.0	100.0	100.0
	0.050	100.0	100.0	100.0	100.0	100.0	100.0	100.0	100.0	100.0	100.0

CHAPTER 6

CONCLUSION

A new model for the V2G frequency regulation operation of an office garage was proposed in this thesis. The proposed model consists of three sub-models: a cost-optimized predictive on-line scheduling model for individual vehicles, a cost-optimized frequency regulation capacity bidding model for an aggregator, and a real-time synergetic dispatch model. The proposed scheduling model for individual vehicles was formulated as a three-stage stochastic linear program, which copes with the uncertainties in 1) energy and frequency regulation prices, and 2) hourly average frequency regulation signal. A near optimal solution procedure was proposed in this thesis to reduce the high computational cost that a traditional multi-stage stochastic linear program encountered. The capacity bidding model for an aggregator coordinates the schedules for individual EVs and the decision for the aggregator. Lastly, the real-time synergetic dispatch model can properly dispatch charge and discharge signals to each individual EVs to protect the battery from extreme SOCs which result in unavailability for frequency regulation. The proposed model is investigated through a simulation of an arbitrary aggregator for an office garage which consists of 100 EVs. The simulation result shows that the computational effort needed by the proposed model is suitable for practical implementation.

REFERENCES

[1]   Medium-term Renewable Energy Market Report, *International Energy Agency*, 2015

[2]   S. W. Hadley, "Impact of plug-in hybrid vehicles on the electric grid," Oak Ridge National Laboratory, Tech Rep., Oct. 2006. [Online]. Available: http://info.ornl.gov/sites/publications/Files/Pub7922.pdf

[3] D. Anair and A. Mahmassani, "State of charge: electric vehicles' global warming emissions and fuel-cost saving across the United States," Union of Concerned Scientists, Jun. 2012

[4]   L. M. Brass, "ORNL study shows hybrid effect on power distribution," news release, Oak Ridge National Lab, Oak Ridge, TN, Mar. 2008

[5]   C. D. White and K.M. Zhange, "Using vehicle-to-grid technology for frequency regulation and peak-load reduction," *Journal of Power Sources*, vol. 196, no. 8, pp. 3972-3980, 2011

[6]   G. Langer, "Poll: traffic in the United States," Feb. 13, 2015, ABC News, [Online], Available: http://abcnews.go.com/technology/traffic/story?id=485098&page=1

[7]   W. Kempton, V. Udo, K. Huber, K. Komara, S. Letendre, S. Baker, D. Brunner and N. Pearre, "A test of vehicle-to-grid for energy storage and frequency regulation in the PJM system", Univ. of Delaware and Pepco Holdings, Inc. , and PJM interconnect and Green Mountain College, 2008

[8]   S. Han, S. Han and K. Sezaki, "Economic assessment on V2G frequency regulation regarding the battery degradation," In *Proc. IEEE ISGT*, Jan 2012, pp. 1-6

[9]   S. Han and S. Han, "Economic feasibility of V2G frequency regulation in consideration of battery wear," *Energies*, vol. 6, no. 2, pp.748-765, 2013

[10]   J. R. Pillai and B. Bak-Jensen, "Integration of vehicle-to-grid in the western Danish power system," *IEEE Trans. Sustainable Energy*, vol. 2, no. 1, pp. 12-19, 2011

[11]   J. R. Pillai and B. Bak-Jensen, "Vehicle-to-grid systems for frequency regulation in an islanded Danish distribution Network," In *Proc. IEEE VPPC*, Sep. 2010, pp 1-6

[12]   P. T. Baboli, M. P. Moghaddam, and F. Fallahi, "Utilizing electric vehicles on primary frequency control in smart power grids," in *Proc. Int. Conf. Petroleum and Sustainable Develop.*, *IPCBEE*, 2011, pp. 6–10

[13]   S. L. Andersson, A. K. Elofsson, M. D. Galus, L. Goransson, S. Karlsson, F. Johnsson, and G. Andersson, "Plug-in hybrid electric vehicles as regulating power providers: case studies of Sweden and Germany," *Energy Policy*, vol. 38, no. 6, pp. 2751-2762, 2010

[14]   J. Kang, S. J. Duncan, and D. N. Mavris, "Real-time scheduling techniques for electric vehicle charging in support of frequency regulation," in *Proc. Comput. Sci.*, vol. 16, no. 0, pp. 767–775, 2013

[15]   Y. Mu, J. Wu, J. Ekanayake, N. Jenkins, and H. Jia, "Primary frequency response from electric vehicles in the Great Britain power system," *IEEE Trans. Smart Grid*, vol. 4, no. 2, pp. 1142–1150, 2013

[16] C. Guille and G. Gross, "A conceptual framework for the vehicle-to-grid (V2G) implementation," *Energy Policy*, vol. 37, no. 11, pp. 4379-4390, 2009

[17] D. Wu, K. T. Chau, and S. Gao, "Multilayer framework for vehicle-togrid operation," in *Proc. IEEE Vehicle Power and Propulsion Conference*, Lille, France, Sep. 2010, pp. 1–6

[18] S. Han, S. H. Han, and K. Sezaki, "Stochastic analysis on the energy constraint of V2G frequency regulation," in *Proc. IEEE VPPC'10*, Sept. 2010

[19] S. Han, S. Han, and K. Sezaki, "Optimal control of the plug-in electric vehicles for V2G frequency regulation using quadratic programming," *IEEE Innovative Smart Grid Technologies*, 1-9 Jan. 2011, pp. 1-6

[20] J. Donadee and M. D. Ilić, "Stochastic co-optimization of charging and frequency regulation by electric vehicles," in *Proc. North Amer. Power Symp.*, Sep. 9–11, 2012, pp. 1–6

[21] J. Donadee and M. D. Ilić, "Stochastic optimization of grid to vehicle frequency regulation capacity bids", *IEEE Trans. Smart Grid*, vol. 5, no. 2, pp. 1061-1069, 2014

[22] E. Yao, V. W. S. Wong and R. Schober, "A robust design of electric vehicle frequency regulation service," in *Proc. IEEE SmartGridComm*, Nov, 2014, pp. 698-703

[23] E. Yao, V. W. S. Wong and R. Schober, "Risk-averse forward contract for electric vehicle frequency regulation service," In *Proc. IEEE SmartGridComm*, 2015, pp. 750-755

[24] E. Yao, V. W. S. Wong and R. Schober, "Robust frequency regulation capacity scheduling algorithm for electric vehicles," *IEEE Tran. Smart Grid*, vol. 8, no. 2, pp. 984-997, 2017

[25]   K. Mets, T. Verschueren, W. Haerick, C. Develder and F. De Turck, "Optimizing smart energy control strategies for plug-in hybrid electric vehicle charging," In *Proc. 12ᵗʰ IEEE/IFIP Network Operations and Management Symposium, 1ˢᵗ IFIP/IEEE international workshop on Management of Smart Grids*, 2010, pp. 293-299

[26]   M. A. Ortega-Vazquez, "Optimal scheduling of electric vehicle charging and vehicle-to-grid services at household level including battery degradation and price uncertainty," *IET Generation, Transmission & Distribution*, vol. 8, no. 6, pp. 1007-1016, 2014

[27]   L. Zhu, F. R. Yu, B. Ning and T. Tang, "Stochastic charging management for plug-in electric vehicles in smart microgrids fueled by renewable energy sources," In *Proc. Online Conference on Green Communication*, 2011, pp. 7-12

[28]   S. Deilami, A. S. Masoum, P. S. Moses and M. A. Masoum, "Real-time coordination of plug-in electric vehicle charging in smart grids to minimize power losses and improve voltage profile," *IEEE Trans. Smart Grid*, vol. 2, no. 3, pp. 456-467. 2011

[29]   T. Kuster, M. Lutzenberger, M. Voß, D. Freund and S. Albayrak, "Applying heuristics and stochastic optimization for load-responsive charging in a smart grid architecture", In *Proc. IEEE PES Innovative Smart Grid Technologies Conference Europe*, 2014, pp. 1-6

[30] A. Di Giorgio, F. Liberati and S. Canale, "Electric vehicles charging control in a smart grid: a model predictive control approach," *Control Engineering Practice*, vol. 22, pp. 147-162, 2014

[31] L. Jian, Y. Zheng, X. Xiao and C. C. Chan, "Optimal scheduling for vehicle-to-grid operation with stochastic connection of plug-in electric vehicles to smart grid," *Applied Energy*, vol. 146, pp. 150-161, 2015

[32] B. Alinia, M. H. Hajiesmaili, and N. Crespi, "Microgrid revenue maximization by charging scheduling of EVs in multiple parking stations," *arXiv Preprint*, *arXiv:1606.01740*, 2016

[33] J. Zhang, X. Wang, K. Men, C. Zhu and S. Zhu, "Aggregation model-based optimization for electric vehicle charging strategy", *IEEE Trans. Smart Grid*, vol. 4, no. 2, pp. 1058-1066, 2013

[34] B. Wang, B. Hu, C. Qiu, P. Chu and P. Gadh, "EV charging algorithm implementation with user price preference," In *Proc. IEEE Power & Energy Society Innovative Smart Grid Technologies Conference*, 2015, pp. 1-5

[35] T. Zhang, W. Chen, Z. Han and Z. Cao, "Charging scheduling of electric vehicle with local renewable energy under uncertain vehicle arrival and grid power price," *IEEE Trans. Vehicular Technology*, vol. 63, no. 6, pp. 2600-2612, 2014

[36] A. Y. Saber and G. K. Venayagamoorthy, "Plug-in vehicles and renewable energy sources for cost and emission reductions," *IEEE Trans. Industrial Electronics*, vol. 58, no. 4, pp. 1229-1238, 2011

[37] D. B. Richardson, "Electric vehicles and the electric grid: a review of modeling approaches, impacts and renewable energy integration," *Renewable and Sustainable Energy Reviews*, vol. 19, pp. 247-254, 2013

[38]   S. Gao, K. Chau, C. Liu, D. Wu and C. C. Chan, "Integrated energy management of plug-in electric vehicles in power grid with renewables," *IEEE Trans. Vehicular Technology*, vol. 63, no. 7, pp. 3019-3027, 2014

[39]   C. Jin, X. Sheng and P. Ghosh, "Optimized electric vehicle charging with intermittent renewable energy sources," *IEEE Journal of Selected Topics in Signal Processing*, vol. 8, no. 6, pp. 1063-1072, 2014

[40]   M. E. Khodayar, L. Wu and M. Shahidehpour, "Hourly coordination of electric vehicle operation and volatile wind power generation in SCUS," *IEEE Trans. Smart Grid*, vol. 3, no. 3, pp. 1271-1279, 2012

[41]   M. Brenna, G. Foiadelli, M. Roscia and D. Zaninelli, "Synergy between renewable sources and electric vehicles for energy integration in distribution systems," In *Proc. IEEE 15th International Conference on Harmonics and Quality of Power,* 2012, pp. 865-869

[42]   A. Damiano, I. Marogniu, M. Porru and A. Serpi, "Electric vehicle energy storage management for renewable energy sources exploitation," In *Proc. IEEE International Electric Vehicle Conference,* 2012, pp. 1-8

[43]   C. Jin, X. Sheng, and P. Ghosh, "Energy efficient algorithms for electric vehicle charging with intermittent renewable energy sources," In *Proc. IEEE PES Power and Energy Society General Meeting*, 2013, pp. 1-5

[44]   J. Traube, F. Lu, D. Maksimovic, J. Mossoba, M. Kromer, P. Faill, S. Katz. B. Borowy, S. Nichols and L. Casey, "Mitigation of solar irradiance intermittency in photovoltaic power

systems with integrated electric-vehicle charging functionality, *IEEE Trans. Power Electronics*, vol. 28, no. 6, pp. 3058-3057, 2013

[45]   C. T. Li, C. Ahn, H. Peng and J. Sun, "Synergistic control of plug-in vehicle charging and wind power scheduling," *IEEE Trans. Power Systems*, vol. 28, no. 2, pp. 1113-1121, 2013

[46]   T. Wu, Q. Yang, Z. Bao and W. Yan, "Coordinated energy dispatching in microgrid with wind power generation and plug-in electric vehicles," *IEEE Trans. Smart Grid*, vol. 4, no. 3, pp. 1453-1463, 2013

[47]   A. Y. Saber and G. K. Venayagamoorithy, "Resource scheduling under uncertainty in a smart grid with renewable and plug-in vehicles," *IEEE Systems Journal*, vol. 6, no. 1, pp. 103-109, 2012

[48]   Y. Li, R. Kaewoyang, P. Wang, D. Niyato and Z. Han, "An energy efficient solution: integrating plug-in hybrid electric vehicle in smart grid with renewable energy," In *Proc. IEEE Conference on Computer Communications Workshops,* 2012, pp. 73-78

[49]   L. Zhu, F. R. Yu, B. Ning and T. Tang, "Optimal charging control for electric vehicles in smart microgrids with renewable energy sources," In *Proc. IEEE 75th Vehicular Technology Conference,* 2012, pp. 1-5

[50]   F. Mwasilu, J. J. Justo, E. K. Kim, T. D. Do and J. W. Jung, "Electric vehicles and smart grid interaction: a review on vehicle to grid and renewable energy sources integration," *Renewable and Sustainable Energy Reviews*, vol. 34, pp. 501-516, 2014

[51]   S. Y. Derakhshandeh, A. S. Masoum, S. Deilami, M. A. Masoum and M. H. Golshan, "Coordination of generation scheduling with PEVs charging in industrial microgirds," *IEEE Trans. Power Systems*, vol. 28, no. 3, pp. 3451-3461, 2013

[52]   R. Anna and D. K. Jain, "Impact of plug-in electric vehicles on the distribution grid," *International Electrical Engineering Journal*, vol. 5, no. 7, pp. 1478-1483, 2014

[53]   G. Cardoso, M. Stadler, M. C. Bozchalui, R. Sharma, C. Marnay, A. Barbosa-Povoa and P. Ferrao, "Optimal investment and scheduling of distributed energy resources with uncertainty in electric vehicle driving schedules," *Energy*, vol. 64, pp. 17-30, 2014

[54]   N. Zou, L. Qian and H. Li, "Auxiliary frequency and voltage regulation in microgrid via intelligent electric vehicle charging," In *Proc. IEEE SmartGridComm*, 2014, pp. 662-667

[55]   H. Liu, Z. Hu, Y. Song and J. Lin, "Decentralized vehicle-to-grid control for primary frequency regulation considering charging demands," *IEEE Trans. Power Systems*, vol. 28, no. 3, pp. 3480-3489, 2013

[56]   H. Yang, C. Y. Chung and J. Zhao, "Application of plug-in electric vehicles to frequency regulation based on distributed signal acquisition via limited communication," *IEEE Trans. Power Systems*, vol. 28, no. 2, pp. 1017-1026, 2013

[57]   M. Datta and T. Senjyu, "Fuzzy control of distributed PV inverters/energy storage systems/electric vehicles for frequency regulation in a large power system," *IEEE Trans. Smart Grid*, vol. 4, no. 1, pp. 479-488, 2013

[58] J. Lin, K. C. Leung and V. O. Li, "Online scheduling for vehicle-to-grid regulation service," In *Proc. IEEE SmartGridComm*, 2013, pp. 43-48

[59] T. Ma and O. Mohammed, "Real-time plug-in electric vehicles charging control for V2G frequency regulation," In *Proc. Annual Conference of IEEE Industrial Electronics Society*, 2013, pp. 1197-1202

[60] J. U. Li, Y. M. Wi, Y. Kim and S. K. Joo, "Optimal coordination of charging and frequency regulation for an electric vehicle aggregator using least square Monte-Carlo (LSMC) with modeling of electricity price uncertainty," *Journal of Electrical Engineering and Technology*, vol. 8, no. 6, pp. 1269-1275, 2013

[61] J. Zhong, L. He, C. Li, Y. Cao, J. Wang, B. Fang, L. Zeng and G. Xiao, "Coordinated control for large-scale EV charging facilities and energy storage devices participating in frequency regulation," *Applied Energy*, vol. 123, pp. 253-262, 2014

[62] S. W. Kim, Y. G. Jin, Y. H. Song and Y. T. Yoon, "Decentralized vehicle-to-grid design for frequency regulation within price-based operation," *Journal Electrical Engineering and Technology*, vol. 10, no. 3, pp. 1335-1341, 2015

[63] J. Tan and L. Wang, "Coordinated optimization of PHEVs for frequency regulation capacity bids using hierarchical game," In *Proc. IEEE Power & Energy Society General Meeting*, 2015, pp. 1-5

[64]   P. Sanchez-Martin, S. Lumbreras and A. Alberdi-Alen, "Stochastic programming applied to EV charging points for energy and reserve service markets," *IEEE Trans. Power Systems*, vol. 31, no. 1, pp. 198-205, 2016

[65]   A. Y. Lam, K. C. Leung and V. O. Li, "Capacity estimation for vehicle-to-grid frequency regulation services with smart charging mechanism," *IEEE Trans. Smart Grid*, vol. 7, no. 1, pp. 156-166, 2016

[66]   C. Peng, J. Zou, L. Lian and L. Li, "An optimal dispatching strategy for V2G aggregator participating in supplementary frequency regulation considering EV driving demand and aggregator's benefits," Applied Energy, vol. 190, pp. 591-599, 2017

[67]   J. Tan and L. Wang, "A game-theoretic framework for vehicle-to-grid frequency regulation considering smart charging mechanism," IEEE Trans. Smart Grid, vol. 8, no. 5, pp. 2358-2369, 2017

[68]   X. Ke, D. Wu, and N. Lu, "A real-time greedy-index dispatching policy for using PEVs to provide frequency regulation service," *IEEE Trans. Smart Grid*, 2017

[69]   H. Han, D. Huang, D. Liu and Q. Li, "Autonomous frequency regulation control of V2G (vehicle-to-grid) system," In *Proc. 19th Chinese Control and Decision Conference*, 2017, pp. 5826-5829

[70]   K. Janfeshan and M. A. Masoum, "Hierarchical supervisory control system for PEVs participating in frequency regulation of smart grids," *Journal of IEEE Power and Energy Technology Systems*, vol. 4, no. 4, pp. 84-93, 2017

[71]   M. Elsis, M. Soliman, M. A. Aboelela and W. Mansour, "Model predictive control of plug-in hybrid electric vehicles for frequency regulation in a smart grid," *IET Generation, Transmission & Distribution*, vol. 11, no. 16, pp. 3974-3983, 2017

[72]   C. Wang, J. Yan, C. Marnay, N. Djilali, E. Dahlquist, J. Wu and H. Jia, "Coordinated control for EV aggregators and power plants in frequency regulation considering time-varying delays", *Applied Energy*, vol. 210 pp. 1363-1376, 2018

[73]   E. Yao, V. W. Wong and R. Schober, "Optimization of aggregate capacity of PEVs for frequency regulation service in day-ahead market," *IEEE Trans. Smart Grid*, vol. 9, no. 4, pp. 3519-3529, 2018

[74]   S. Han, S. Han and K. Sezaki, "Development of an optimal vehicle-to-grid aggregator for frequency regulation," *IEEE Trans. Smart Grid*, vol.1, no. 1, pp. 65-72, 2010

[75]   E. Sortomme and M. A. El-Sharkawi, "Optimal scheduling of vehicle-to-grid energy and ancillary services," *IEEE Trans. Smart Grid*, vol. 3, no. 1, pp. 351-359, 2012

[76]   M. G. Vaya and G. Andersson, "Combined smart-charging and frequency regulation for fleets of plug-in electric vehicles," in *Proc. IEEE Power Energy Soc. Meeting*, Vancouver, BC, Canada, Jul. 2013, pp. 1–5

[77]   R. Wang, Y. Li, P. Wang, and D. Niyato, "Design of a V2G aggregator to optimize PHEV charging and frequency regulation control," in *Proc. IEEE Int. Conf. Smart Grid Commun.*, Oct. 2013, pp. 127–132

[78] J. J. Escudero-Garzas, A. Garcia-Armada and G. Seco-Granados, "Fair design of plug-in electric vehicles aggregator for V2G regulation," *IEEE Tran. Vehicular Tech*. vol.6, no. 8, pp. 3406-3419, 2012

[79] PJM Manual 12, PJM ISO, May 1, 2017. [Online]. Available: http://pjm.com/~/media/documents/manuals/m12.ashx

[80] PJM Manual 28, PJM ISO, May 1, 2017. [Online]. Available: http://pjm.com/~/media/documents/manuals/m28.ashx

[81] RTO regulation signal data, PJM ISO, Feb. 2, 2016. [Online]. Available: http://www.pjm.com/~/media/markets-ops/ancillary/mkt-based-regulation/regulation-data.ashx

[82] A. Madansky, "Inequalities for stochastic linear programming problems," *Management Science*, vol. 6, pp. 197-204, 1960

[83] L. Sanna, "Driving the solution, the plug-in hybrid vehicle," *EPRI Journal*, 2005, pp. 8-17

[84] PJM regulation zone preliminary billing data, PJM ISO, Feb. 2, 2016. [Online]. Available: http://www.pjm.com/markets-and-operations/billing-settlements-and-credit/preliminary-billing-reports/pjm-reg-data.aspx

[85] Hourly real-time and day-ahead LMP, PJM ISO, Feb. 2, 2016. [Online]. Available: http://www.pjm.com/markets-and-operations/energy/real-time/monthlylmp.aspx

[86] G. B. Dantzig and P. Wolfe, "Decomposition principle for linear programs," *Operations Research*, 1960, vol. 8, no. 1, pp. 101-111

[87]   V. Chankong, "Optimality tests for partitioning and sectional search algorithms," *Applied*

Mathematics & Computation, 1991, vol. 44, no. 2, pp. 157-182